

2021

## The Role of Oxygen in Stimulating Methane Production in Wetlands

Jared L. Wilmoth

Jeffra K. Schaefer


Danielle R. Schlesinger

Spencer W. Roth

Patrick G. Hatcher

*See next page for additional authors*

Follow this and additional works at: [https://digitalcommons.odu.edu/chemistry\\_fac\\_pubs](https://digitalcommons.odu.edu/chemistry_fac_pubs)

 Part of the [Atmospheric Sciences Commons](#), [Climate Commons](#), and the [Environmental Chemistry Commons](#)

---

### Original Publication Citation

Wilmoth, J. L., Schaefer, J. K., Schlesinger, D. R., Roth, S. W., Hatcher, P. G., Shoemaker, J. K., & Zhang, X. N. (2021). The role of oxygen in stimulating methane production in wetlands. *Global Change Biology*, 27(22), 5831-5847. <https://doi.org/10.1111/gcb.15831>

This Article is brought to you for free and open access by the Chemistry & Biochemistry at ODU Digital Commons. It has been accepted for inclusion in Chemistry & Biochemistry Faculty Publications by an authorized administrator of ODU Digital Commons. For more information, please contact [digitalcommons@odu.edu](mailto:digitalcommons@odu.edu).

---

**Authors**

Jared L. Wilmoth, Jeffra K. Schaefer, Danielle R. Schlesinger, Spencer W. Roth, Patrick G. Hatcher, Julie K. Shoemaker, and Xinning Zhang

## PRIMARY RESEARCH ARTICLE

# The role of oxygen in stimulating methane production in wetlands

Jared L. Wilmoth<sup>1</sup> | Jeffra K. Schaefer<sup>2</sup>  | Danielle R. Schlesinger<sup>3</sup>  |  
Spencer W. Roth<sup>2</sup>  | Patrick G. Hatcher<sup>4</sup> | Julie K. Shoemaker<sup>5</sup> | Xinning Zhang<sup>1,3</sup> 

<sup>1</sup>High Meadows Environmental Institute, Princeton University, Princeton, NJ, USA

<sup>2</sup>Department of Environmental Sciences, Rutgers University, New Brunswick, NJ, USA

<sup>3</sup>Department of Geosciences, Princeton University, Princeton, NJ, USA

<sup>4</sup>Natural Sciences and Mathematics, Lesley University, Cambridge, MA, USA

<sup>5</sup>Department of Chemistry and Biochemistry, Old Dominion University, Norfolk, VA, USA

## Correspondence

Xinning Zhang, High Meadows Environmental Institute, Princeton University, Princeton, NJ 08544, USA.  
Email: xinningz@princeton.edu

## Funding information

U.S. National Science Foundation Graduate Research Fellowship, Grant/Award Number: DGE 1842213; U.S. Department of Energy-Geosciences, Grant/Award Number: DE-FG02-94ER14466; U.S. National Science Foundation, Grant/Award Number: CHE-1610021; Carbon Mitigation Initiative, High Meadows Environmental Institute, Princeton University; U.S. National Science Foundation - Earth Sciences, Grant/Award Number: EAR-1128799

## Abstract

Methane (CH<sub>4</sub>), a potent greenhouse gas, is the second most important greenhouse gas contributor to climate change after carbon dioxide (CO<sub>2</sub>). The biological emissions of CH<sub>4</sub> from wetlands are a major uncertainty in CH<sub>4</sub> budgets. Microbial methanogenesis by Archaea is an anaerobic process accounting for most biological CH<sub>4</sub> production in nature, yet recent observations indicate that large emissions can originate from oxygenated or frequently oxygenated wetland soil layers. To determine how oxygen (O<sub>2</sub>) can stimulate CH<sub>4</sub> emissions, we used incubations of *Sphagnum* peat to demonstrate that the temporary exposure of peat to O<sub>2</sub> can increase CH<sub>4</sub> yields up to 2000-fold during subsequent anoxic conditions relative to peat without O<sub>2</sub> exposure. Geochemical (including ion cyclotron resonance mass spectrometry, X-ray absorbance spectroscopy) and microbiome (16S rDNA amplicons, metagenomics) analyses of peat showed that higher CH<sub>4</sub> yields of redox-oscillated peat were due to functional shifts in the peat microbiome arising during redox oscillation that enhanced peat carbon (C) degradation. *Novosphingobium* species with O<sub>2</sub>-dependent aromatic oxygenase genes increased greatly in relative abundance during the oxygenation period in redox-oscillated peat compared to anoxic controls. *Acidobacteria* species were particularly important for anaerobic processing of peat C, including in the production of methanogenic substrates H<sub>2</sub> and CO<sub>2</sub>. Higher CO<sub>2</sub> production during the anoxic phase of redox-oscillated peat stimulated hydrogenotrophic CH<sub>4</sub> production by *Methanobacterium* species. The persistence of reduced iron (Fe(II)) during prolonged oxygenation in redox-oscillated peat may further enhance C degradation through abiotic mechanisms (e.g., Fenton reactions). The results indicate that specific functional shifts in the peat microbiome underlie O<sub>2</sub> enhancement of CH<sub>4</sub> production in acidic, *Sphagnum*-rich wetland soils. They also imply that understanding microbial dynamics spanning temporal and spatial redox transitions in peatlands is critical for constraining CH<sub>4</sub> budgets; predicting feedbacks between climate change, hydrologic variability, and wetland CH<sub>4</sub> emissions; and guiding wetland C management strategies.

This is an open access article under the terms of the Creative Commons Attribution-NonCommercial-NoDerivs License, which permits use and distribution in any medium, provided the original work is properly cited, the use is non-commercial and no modifications or adaptations are made.

© 2021 The Authors. *Global Change Biology* published by John Wiley & Sons Ltd.

## KEYWORDS

carbon mitigation, carbon-climate feedback, climate change, peatland microbiome, soil microbial carbon cycling, soil redox dynamics, wetland management, wetland methane

## 1 | INTRODUCTION

Wetlands are a large and highly variable natural source of methane ( $\text{CH}_4$ ), the second most important greenhouse gas contributing to climate change after  $\text{CO}_2$  (Dean et al., 2018). The rapid increase in atmospheric  $\text{CH}_4$  concentrations since 2007 may be caused by wetlands (Dean et al., 2018; Turner et al., 2019; Zhang et al., 2017). Wetland processes are thought to be important in positive carbon (C)-climate feedbacks, as the large fraction of global soil C stored in high latitude and tropical peats is vulnerable to microbial release as  $\text{CH}_4$  and carbon dioxide ( $\text{CO}_2$ ) with continued warming (Dean et al., 2018; Loisel et al., 2021). A mechanistic understanding of the interplay between hydrological, microbial, and plant-associated processes in shaping wetland  $\text{CH}_4$  emissions is required to decipher current trends and improve projections.

Wetland  $\text{CH}_4$  is produced by methanogens, anaerobic microorganisms in the domain Archaea (Dean et al., 2018). Because oxygen ( $\text{O}_2$ ) inhibits  $\text{CH}_4$  production upon direct exposure to methanogen cells (Thauer et al., 2008), much of the previous research on  $\text{CH}_4$  emissions from wetlands has focused on permanently saturated, fully anoxic peat below the water table where most organic carbon (OC) is stored (Dean et al., 2018). However, more recent studies have indicated that the highest  $\text{CH}_4$  emissions from several wetland/wet soils arise from redox-oscillating and/or oxygenated, near-surface layers (e.g., Angle et al., 2017; Clymo et al., 1995; Longhi et al., 2016; Shoemaker & Schrag, 2010; Shoemaker et al., 2012; Teh et al., 2005; Turetsky et al., 2014; Yang et al., 2017). In some cases, the near-surface layers have been estimated to contribute as much as ~80% of wetland  $\text{CH}_4$  emissions (Angle et al., 2017; Shoemaker et al., 2012). To help explain the paradox of  $\text{O}_2$ -associated  $\text{CH}_4$  production, local (e.g., within soil microsites) and temporal anoxia have been proposed to arise within the uppermost fraction of the saturated zone and in unsaturated top layers (Angle et al., 2017; Clymo et al., 1995; Shoemaker & Schrag, 2010; Shoemaker et al., 2012; Teh et al., 2005; Yang et al., 2017). While the presence of anoxic microsites in frequently oxygenated wetland soils may provide an environment where anaerobic processes could occur (Keiluweit et al., 2016, 2018; Teh et al., 2005), it remains unclear why methanogenesis in the shallow oxygenated layers would be more active than in deeper, persistently anoxic layers.

Peat is particularly rich in aromatic and polyphenolic compounds (Hodgkins et al., 2016), which can be efficiently degraded by the aromatic oxidase enzymes of certain aerobic microorganisms with  $\text{O}_2$  serving as both a co-substrate for oxygenase activity and as the terminal electron acceptor for respiration (Fenner & Freeman, 2011; Freeman et al., 2001, 2004; Sinsabaugh, 2010). Soluble and condensed polyphenols (e.g., tannin-like compounds) have been shown to display enzymatic inhibition in different

systems by directly binding to microbial enzymes and blocking their function (Bhat et al., 1998; Field & Lettinga, 1987, 1992). These observations have led to the proposal that such compounds act as a biogeochemical barrier (or latch) on anaerobic microbial organic C degradation to  $\text{CO}_2$  and  $\text{CH}_4$  in peatlands and thus are critical controls on C storage (Fenner & Freeman, 2011; Freeman et al., 2004). In this view, soils that undergo drought cycles would exhibit reduced C storage and enhanced greenhouse gas emissions under drought recovery, as temporary exposures of  $\text{O}_2$  during drought could reduce the inhibitory effects of polyphenols on microbial activity (Fenner & Freeman, 2011; Freeman et al., 2004). However, it has also been demonstrated that wetland soil microbial communities can degrade tannin, a model polyphenol, under anoxic conditions (McGivern et al., 2021) and the presence of tannin-like compounds in wetland and forest soils can actually increase microbial enzymatic activity (Adamczyk et al., 2017; Bengtsson et al., 2018; McGivern et al., 2021). The toxicity and regulatory role of polyphenols has been further called into question by studies (e.g., Bengtsson et al., 2018; Brouns et al., 2014; Zak et al., 2019) that collectively suggest that factors such as the microbial activities of specific polyphenolic compounds and nutrient availability could be highly important in determining C mineralization pathways in *Sphagnum* peat.

Thus, a more fundamental cause of  $\text{O}_2$ -enhanced  $\text{CH}_4$  production could be that  $\text{O}_2$ , as a co-substrate of specific microbial enzymes involved in organic C breakdown and a high redox potential terminal electron acceptor, allows microbial communities to obtain more nutrients and energy from complex organic C (Keiluweit et al., 2016, 2018; LaRowe & Cappellen, 2011; Lehmann & Kleber, 2015; Schmidt et al., 2011). Following this framework, we expect that  $\text{O}_2$  can enable the proliferation of aerobic microbes equipped with enzymes (e.g., aromatic oxygenases) that allow degradation of OC in complex, less bioavailable OC pools, including the larger polyphenols (Figure 1 step 1). The high activity of polyphenolic C-degrading aerobes would enable greater conversion of peat OC into smaller C and energy forms such as sugars, organic acids,  $\text{H}_2$ , and  $\text{CO}_2$  that are more bioavailable for the anaerobic food web and methanogenesis (Meronigal et al., 2003) under subsequent (temporal) or neighboring (spatial) anoxic conditions (Figure 1 steps 2 and 3). In addition to microbial processes, it is also possible that abiotic mechanisms related to iron (Fe) redox cycling may contribute to organic C degradation in peat subject to spatiotemporal  $\text{O}_2$  changes. The co-occurrence of Fe(II) species and  $\text{O}_2$  may lead to Fenton-like reactions that generate hydroxyl radicals to oxidize organic C (Page et al., 2013; Trusiak et al., 2018) and thereby stimulate downstream C processing toward methanogenesis.

In this study, we investigated the following question based on recent field and laboratory observations: What are the primary

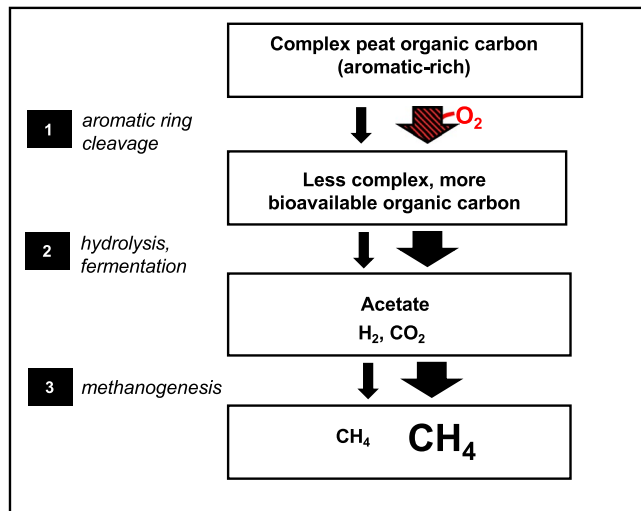


**FIGURE 1** Proposed mechanism showing effects of spatiotemporal oxic-anoxic transitions on microbial degradation of peat to  $\text{CH}_4$ .  $\text{O}_2$  exposure promotes efficient degradation of aromatic, phenolic peat constituents (step 1), which enhances peat carbon bioavailability during anoxic processing into methanogenic precursors (step 2), to stimulate methanogenesis (step 3). Red hatched arrow indicates processes directly involving  $\text{O}_2$ , solid black arrows indicate anaerobic processes

biogeochemical controls that could allow  $\text{O}_2$  to stimulate  $\text{CH}_4$  production in wetlands? Our hypothesis, informed by the framework described in Figure 1, was that  $\text{O}_2$  transitions allow for the partitioning (i.e., temporal or spatial) of specific aerobic and anaerobic pathways that collectively function to increase the production of methanogenic substrates and thus lead to higher  $\text{CH}_4$  emissions. To identify both biotic and abiotic mechanisms, we compared geochemical, high-resolution mass spectrometry, omics, and synchrotron characterizations of laboratory incubations of *Sphagnum* peat temporarily exposed to  $\text{O}_2$  followed by incubation under anoxic conditions to peat kept continuously anoxic over the course of ~8 months. Our results confirm that transient oxygenation of peat enhances anaerobic  $\text{CH}_4$  production by orders of magnitude compared to peat that remains continuously anoxic, which supports and broadens the results of earlier work (Brouns et al., 2014). By using a combined geochemical and microbial sequencing approach, we identify specific biological mechanisms whereby  $\text{O}_2$ -enhanced methanogenesis in acidic peat results from the coupling of microbial functions spanning a redox transition, which perpetuates organic C mineralization and leads to increased hydrogenotrophic  $\text{CH}_4$  emissions. The biogeochemical steps characterized in this mechanism can help resolve the paradox of large  $\text{CH}_4$  emissions from shallow, oxygenated wet soil (Angle et al., 2017; Longhi et al., 2016; O'Connell et al., 2018; Shoemaker & Schrag, 2010; Shoemaker et al., 2012; Teh et al., 2005; Turetsky et al., 2014; Turetsky et al., 2014; Yang et al., 2017), explain potential positive C-climate feedbacks (O'Connell et al., 2018), and guide wetland C management strategies (Abdalla et al., 2016).

## 2 | MATERIALS AND METHODS

### 2.1 | Field sampling and site description

Peat samples, primarily composed of *Sphagnum* vegetation, were collected from the Ward Reservation (Andover, MA, USA, 42°38'N 71°06'W), a site comprised of wetlands, lakes, woodlands and fields, based on differences in the extent of natural degradation, which was qualitatively assessed using profile depth and color gradient changes. Slices of peat were removed from three different depths within a *Sphagnum* hummock and hollow feature: 0–5 cm below the water table ("BWT" layer peat), 0–5 cm above the water table ("AWT" layer peat), and 5–10 cm above the water table ("UNS" layer peat). Peat from above the water table was sealed in ziplock bags; BWT peat was packed into 1-L glass jars and remaining air gaps were filled with overlying surface water from the hollow. Peat and associated pore waters were stored on ice and transported to the laboratory for immediate processing.

### 2.2 | Incubations

Peat slurry incubations were prepared by blending peat of a specific layer (300 g wet weight) with a 10% v/v dilution of site water (0.2  $\mu\text{m}$  filtered site water diluted in  $\text{N}_2$ -purged DI water) to a final 1 L slurry volume while continuously flushing with  $\text{N}_2$  gas to minimize oxidation and deoxygenate the slurry (Hines et al., 2008). For a given layer of peat, slurry aliquots (90 ml) from the same batch of prepared slurry were dispensed into glass serum bottles (160 ml) under  $\text{N}_2$ , sealed with butyl septum stoppers (20 mm, Bellco Glass), and covered with aluminum foil. Incubations of each peat layer (BWT, AWT, and UNS) were then subjected to 0%, 5%, and 10% v/v  $\text{O}_2$  treatments, with each treatment performed in triplicate. Because preliminary treatment of incubations with  $\text{O}_2$  indicated that flushing needed to occur at least every 3 days to prevent complete consumption of added  $\text{O}_2$ ,  $\text{O}_2$  treatments were maintained during the incubation by flushing the headspace of serum bottles (headspace replaced at least six times) with filled 60-ml syringes containing either 5%  $\text{O}_2$  + 95%  $\text{N}_2$  or 10%  $\text{O}_2$  + 90%  $\text{N}_2$  using analytical grade air (to supply  $\text{O}_2$ ) and 100%  $\text{N}_2$  gas (ultrahigh purity) every 2–3 days over a 98-day period. Incubations were shaken on their sides at 150 rpm at room temperature in the dark to ensure even distribution of headspace gases throughout the liquid slurry. Following 98 days of incubation, all serum bottles were flushed with 100%  $\text{N}_2$  followed by incubation for an additional 134 days under anoxic conditions with no headspace flushing (total incubation of 232 days). A set of shorter term, 1-month long slurry incubations with BWT peat were performed with 0% and 21% v/v  $\text{O}_2$  treatment for 1 week by daily flushing of headspace with air followed by 3 weeks of anoxia under the same temperature and shaking conditions as long-term incubations. Subsamples of headspace gases (3 ml) from long-term incubations were collected with 5-ml sterile Luer lock syringes (BD) and sterile 22 gauge needles (BD); peat slurry subsamples (4 ml) were collected

with 5-ml sterile Luer lock syringes and sterile 16 gauge, wide-bore needles (to prevent clogging) at days 21, 98, 126, 198, and 232. Gas and slurry samples from days 21 and 98 were collected from incubations prior to headspace flushing. The sample volumes removed from the incubations were balanced by addition of the appropriate gas mixture, and the headspace dilution was used to calculate final gas concentrations. Headspace gas from short-term incubations was collected every 2–6 days following the above procedure for long-term incubations. In preparation for later chemical analyses, gas samples were stored at  $-20^{\circ}\text{C}$  in 5-ml amber glass vials that had been previously sealed, flushed with  $\text{N}_2$ , and evacuated by vacuum. Processing of slurry aliquots occurred quickly under limited ambient headspace immediately after sampling, where the aqueous phase of slurries was first separated from solid peat by centrifugation at 10,000 g for 15 min and filtered through 0.2- $\mu\text{m}$  pore-size syringe filters (Agilent, Captiva Premium Syringe filter, PTFE, 15 mm) into acid-washed, methanol-cleaned amber glass vials. Liquid and solid peat phases were stored at  $-20^{\circ}\text{C}$  until further analysis. Peat samples were preserved in LifeGuard Soil Preservation solution (QIAGEN) and stored at  $-20^{\circ}\text{C}$  for later nucleic acid extraction. All stored gas, aqueous, and solid samples were analyzed following the conclusion of the 232-day incubation experiment within 1 week (gas) or in a couple of months (aqueous, solid).

### 2.3 | Gas, dissolved organic carbon (DOC) and volatile fatty acid (VFA) measurements

Methane ( $\text{CH}_4$ ) concentrations were determined by injecting a diluted 1 ml aliquot of sampled incubation headspace gas into a Shimadzu GC-8A gas chromatograph equipped with a Supelco 80/100 HAYESEP N column and flame ionization detector. The remaining 2 ml headspace sample was used to measure the concentrations of  $\text{H}_2$  and  $\text{CO}_2$  on a Shimadzu GC-8A gas chromatograph equipped with a Restek ShinCarbon ST column and thermal conductivity detector. The concentration of total dissolved organic carbon (DOC) in filtered aqueous samples was measured on a Shimadzu TOC-V CSN analyzer. The concentrations of volatile fatty acids (VFAs) were measured on an Agilent HPLC equipped with Bio-Rad Aminex HPX-87H (300 mm  $\times$  7.8 mm) column for acetate, propionate, and butyrate detection by UV.

### 2.4 | Fourier transform ion cyclotron resonance mass spectrometry (FT-ICR-MS)

Filtered aqueous samples (4 ml) of peat slurry DOC were analyzed by FT-ICR-MS using the method of Ohno et al. (2016). Briefly, filtrates were first processed through Agilent PPL solid-phase extraction cartridges (Agilent Bond Elut) to desalt the samples. Prepared DOC samples were then diluted with methanol and analyzed in the negative ion mode using an Apollo II electrospray ionization source of a Bruker Daltonics 12 T Apex Qe FT-ICR-MS (Sleighter & Hatcher,

2008) at the College of Sciences Major Instrumentation Cluster laboratory at Old Dominion University. Samples were introduced by a syringe pump providing an infusion rate of  $120 \mu\text{l h}^{-1}$  and analyzed with the electrospray voltages optimized for each sample in order to maintain consistent and stable ion currents. Ions between 200 and 1200 m/z were accumulated in a hexapole for 1.0 s before being transferred to the ICR cell. The summed free induction decay signal was zero-filled once and Sine-Bell apodized prior to fast Fourier transformation and magnitude calculation using the Bruker Daltonics Data Analysis software. To assign unique molecular formulae from 200 to 1200 m/z, an in-house MATLAB script written at Old Dominion University was used according to the following criteria:  $^{12}\text{C}_{2-50}$ ,  $^1\text{H}_{5-100}$ ,  $^{14}\text{N}_{0-6}$ ,  $^{16}\text{O}_{1-30}$ ,  $^{32}\text{S}_{0-2}$ , and  $^{31}\text{P}_{0-2}$  within an error of 1 ppm (Didonato et al., 2016). For data analyses, the detection (presence or absence) of compounds was used to report average changes in molecular species characteristics over time (e.g., aromaticity index (AI), nominal oxidation state of carbon (NOSC), exact mass, H/C ratio versus O/C ratio, and double bond equivalency per C (DBE/C); Pracht et al., 2018). The relative intensities of all detected compounds were used in a principal component analysis (PCA) to assess the loadings of individual molecules on the PC axes (Hawkes et al., 2016) in a comparison of weighted molecular species characteristics to those investigated based only on the presence or absence of compounds. We note that calculations based on FT-ICR-MS detection and/or relative intensities provide an approximation of the molecular composition of a given sample when considering that (1) ionization efficiencies are not equal across different compounds, which could impact both the relative intensities and the final presence or absence of compounds, and (2) only molecules within the overall m/z range of 200–1200 are finally measured, which excludes small and large molecules that fall outside this range. However, analyses based on peak intensities can still provide useful information on relative changes in composition between similar sample types (e.g., samples across a time course as here) that have been manipulated and analyzed in the same way (e.g., Sleighter et al., 2012; Wozniak et al., 2020).

### 2.5 | X-ray absorbance spectroscopy

Solid peat samples were analyzed for iron (Fe) oxidation state on the Submicron Resolution X-ray Spectroscopy beamline at sector 5-ID at the National Synchrotron Light Source II at Brookhaven National Laboratory. Each sample was mounted between Kapton tape. A map (20  $\mu\text{m}^2$  with a 2  $\mu\text{m}$  step size, 2.0 s/point acquisition time) was made at the Fe k-edge in order to search for Fe hotspots in each sample. Fe XANES were run at selected spots from  $-100$  to  $-10$  eV below the Fe k-edge (step size 5.0 eV), from  $-10$  eV below to 70 eV above the Fe k-edge (0.2 eV step size), and 70 to 120 eV above the Fe k-edge (5.0 eV step size) with a 2.0 sec/point acquisition time. Fe XANES standard spectra of aqueous Fe(II)-sulfate and Fe(III)-nitrate were collected at the beamline and were used to calibrate all samples to the same Fe k-edge energy (Von Der Heyden et al., 2017). The fit

error for the Fe XANES Fe(II) species versus Fe(III) species was  $\pm 3\%$  for the percentage of each species. All spectra were analyzed using Athena (Ravel & Newville, 2005a, 2005b). Spectra were normalized by fitting a first-order polynomial to the pre-edge region and by fitting a first- or second-order polynomial to normalize the post-edge region to 1.0. Normalized spectra were fit to Fe standards using linear combination fitting in order to determine the relative percentages of Fe(II) versus Fe(III); Non Der Heyden et al., 2017).

## 2.6 | Nucleic acid extraction, 16S rRNA gene amplicon and metagenomic sequence analyses

Total nucleic acids from peat slurries (6 ml of combined slurry from replicates sampled before 232 days, 6 ml of slurry per replicate sampled at 232 days) were extracted with the RNeasy PowerSoil Total RNA kit (QIAGEN). Purified DNA was eluted with the PowerSoil DNA Elution kit (QIAGEN) and used for 16S rRNA gene amplicon and metagenomic sequencing performed at Molecular Research LP (MR DNA). The V4 region of the 16S rDNA gene was sequenced using the 515F and 806R primers on the Illumina MiSeq platform to generate 50,000 read pairs per sample using 250-nt paired ends. 16S amplicon sequences were processed using QIIME2 version 2018.11 (Caporaso et al., 2010). Sequences were demultiplexed, barcodes and adapter sequences were removed, and paired-end sequences were joined. Quality filtering was carried out with q-score plugin and features were assigned using Deblur (Amir et al., 2017). Taxonomy was assigned using a feature-classifier (Pedregosa et al., 2011) trained on the V4 region of the Silva release 132 99% database. Sequences were aligned with MAFFT and a phylogenetic tree for diversity analyses was created with Fasttree 2 (Price et al., 2010). Rarefaction and beta-diversity analyses of sequences were performed using weighted and unweighted UniFrac metrics (Lozupone et al., 2006). The significance of beta-diversity between O<sub>2</sub> treatments was determined with a nonparametric permutation-based analysis in QIIME2.

Metagenomic DNA was sequenced on the Illumina HiSeq platform to generate  $1 \times 10^7$  read pairs per sample using 150-nt paired ends. Sequence quality and downstream processing were evaluated with FastQC (Brown et al., 2017). Sequences were joined (merged) with PEAR, and Trimmomatic was used to remove Illumina adapter and barcode sequences (Bolger et al., 2014; Zhang et al., 2014). Processed metagenomic reads were then searched against the current NCBI RefSeq proteins database using DIAMOND with BlastX searches and an E-value cutoff of  $10^{-3}$  (Buchfink et al., 2015). Significantly matched reads to the RefSeq database were then analyzed in the current version of MEGAN (Community Edition) to assign taxonomic and functional annotations (Huson et al., 2016). Functionally assigned reads were grouped by SEED classifications and assembled contigs from different groups were further evaluated using BlastX and Interpro scans (Huson et al., 2016). Principal coordinate analysis (PCA) of read counts based on both taxonomy and function was performed in R using Bray–Curtis distances.

Sequence data for this project have been deposited at NCBI under SRA accession PRJNA551662.

## 2.7 | *mcrA* qPCR

Quantitative PCR analyses of the methyl coenzyme M reductase gene (*mcrA*) in DNA from peat slurries were performed using primers *mlas* and *mcrA-rev* (Angle et al., 2017; Franchini et al., 2014). Amplification reactions contained QuantiNova SYBR Green reagents (QIAGEN), 2  $\mu$ l template, with all other reagent concentrations and volumes as previously reported (Angle et al., 2017; Franchini et al., 2014). Thermocycler (Stratagene Mx3000P) settings were 3 min at 95°C, followed by 40 cycles of 95°C for 25 s, 55°C for 45 s, 72°C for 30 s, and finally 78°C for 30 s. The *mcrA* gene sequence of *Methanobacterium subterraneum* strain A8p (NCBI genome accession: NZ\_CP017768.1; NCBI sequence ID: WP\_100905596.1) was used as the standard.

## 3 | RESULTS AND DISCUSSION

### 3.1 | Transient O<sub>2</sub> exposure stimulates anaerobic CH<sub>4</sub> production

The incubations of slurried peat, containing *Sphagnum* vegetation from an acidic northeastern wetland exhibiting different degrees of degradation, as assessed by depth and color (Figure 2a), were exposed to variable concentrations of oxygen for 98 days (~3 months) by flushing with 0%, 5%, or 10% O<sub>2</sub> gas every 2 to 3 days, followed by incubation under anoxic conditions for a subsequent 134 days (~4.5 months) to result in a total incubation duration of 232 days. The incubation intervals were primarily selected to test the effects of redox transition on net CH<sub>4</sub> production following prolonged exposure to O<sub>2</sub> under laboratory conditions. However, this incubation design may be useful for conceptualizing how environmental changes in redox status related to seasonal changes in the water table depth, long-term diffusion dynamics in peat, or engineered shifts in wetland oxygenation influence CH<sub>4</sub> emissions (Duddleston et al., 2002; Fan et al., 2014; Jørgensen et al., 2012). We found that every peat sample exposed to O<sub>2</sub> yielded dramatically higher CH<sub>4</sub> levels by the end of the anoxic phase of incubation compared to samples kept continuously anoxic (Figure 2b). The largest increases in CH<sub>4</sub> production (~1,000–2,000 fold) were observed for moderately and highly degraded brown, fibrous peat material collected within 5 cm of the water table (the “at water table” AWT and “below water table” BWT layers, respectively, Figure 2a). In complementary shorter term experiments, the transient exposure of degraded peat to 21% O<sub>2</sub> for 1 week followed by anoxic incubation for 3 weeks also induced a rise in CH<sub>4</sub> yield (~30-fold) compared to continuously anoxic peats (Figure S1), results generally consistent with previous observations of a sevenfold increase in CH<sub>4</sub> production rate from peat incubations following 1 week of oxygenation (Brouns et al., 2014).

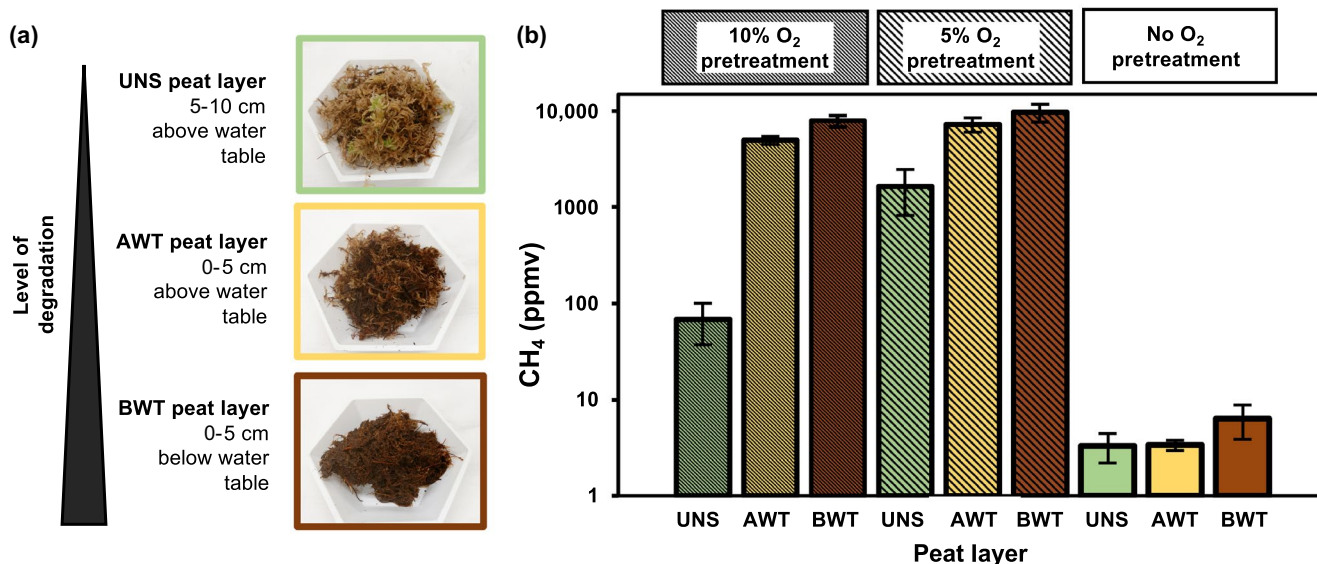


**FIGURE 2** Effect of  $O_2$  pretreatment on methane yields from anoxic slurry incubations of different peat layers at the end of the incubation experiment (232 days). (a) Incubations contained fresh (UNS for unsaturated peat, dark green bar), moderately degraded (AWT for at water table peat, light orange bar), or highly degraded *Sphagnum* peat (BWT for below water table, dark brown bar) sampled from different depths of a temperate wetland. (b) Methane yields from incubations of peat layers exposed to 10% or 5%  $O_2$  for 98 days prior to anoxic incubation for a subsequent 134 days (hatched bars) and from incubations kept continuously anoxic for 232 days (solid bars). Error bars represent the standard errors of  $n = 2$  or 3 biological replicates

### 3.2 | Changes in peat chemistry

To elucidate the role of  $O_2$  pre-exposure in promoting anaerobic  $CH_4$  production, we studied changes in the decomposition of complex organic matter by measuring DOC and headspace gases (Figure 3; Figures S2–S4; Table S1; Data S1), focusing on incubations of moderately and deeply degraded peat (AWT, BWT layers), which showed the largest  $CH_4$  yields (Figure 2). The anaerobic decomposition of large, complex organic C molecules is an inefficient, stepwise process compared to that occurring under aerobic conditions due to kinetic and thermodynamic limitations (Dean et al., 2018; Kristensen et al., 1995; LaRowe & Cappellen, 2011; Lehmann & Kleber, 2015; Megonigal et al., 2003). An important determinant of decomposition efficiency is the initial conversion of C in large, polymeric compounds into more bioavailable forms (Figure 1, step 1; Lehmann & Kleber, 2015; Megonigal et al., 2003; Wakeham & Canuel, 2006). This initial step in anoxic systems can be very slow without the efficient breakdown of large compounds first being stimulated by  $O_2$  and the requisite microbial enzymes (Fenner & Freeman, 2011; Wakeham & Canuel, 2006). Subsequent anaerobic hydrolysis of polymers into monomers and fermentation of monomeric C (Figure 1, step 2) produce more bioavailable substrates like hydrogen ( $H_2$ ), carbon dioxide ( $CO_2$ ) and acetate ( $CH_3COO^-$ ) that can directly fuel methanogenesis (Figure 1, step 3; Megonigal et al., 2003).

Consistent with the well-accepted role of  $O_2$  in enabling efficient C mineralization (Wakeham & Canuel, 2006), we measured much lower DOC and higher  $CO_2$  levels in  $O_2$ -treated peat samples compared to those that remained anoxic (Figure 3a,b,e,f; Figure S2). Oxidic conditions reduced DOC concentrations by roughly half, while

anoxic conditions led to DOC accumulation (Figure 3a,b). The  $O_2$ -treated samples continued to exhibit higher  $CO_2$  levels compared to untreated samples, even during the later anoxic incubation phase (Figure 3e,f). This result indicates that prior  $O_2$  exposure enhances subsequent anaerobic processes.

Three pathways distinguished by different substrates are mainly responsible for biological  $CH_4$  production (Megonigal et al., 2003): hydrogenotrophic methanogenesis, which requires both  $CO_2$  and  $H_2$  ( $CO_2 + 4 H_2 \rightarrow CH_4 + 2H_2O$ ), acetoclastic methanogenesis which requires acetate ( $CH_3COOH \rightarrow CH_4 + CO_2$ ), and methylotrophic methanogenesis involving one-carbon (C1) compounds such as methanol. All of these routes require common fermentation products as substrates (Figure 1). We observed  $H_2$  levels that were conspicuously low during the anoxic period in  $O_2$ -pretreated peat samples relative to levels in continuously anoxic peat samples (Figure 3g,h; Figure S2). This result most likely reflects the large  $H_2$  consumption by hydrogenotrophic methanogenesis that was enabled by the high  $CO_2$  levels from  $O_2$  enhancement of anaerobic degradation (Figure 3e), favoring higher  $CH_4$  levels by the end of the incubation (Figure 3i).  $O_2$  inhibition of  $H_2$ -producing anaerobic fermentations could also explain the low  $H_2$  levels during the oxic period (Figure 3g; Figure S2). In contrast, higher  $H_2$  concentrations in continuously anoxic peats (Figure 3h) indicate active fermentation of more bioavailable forms of DOC, which releases acetate and  $H_2$ , but relatively small amounts of  $CO_2$  for hydrogenotrophic methanogenesis (Figure 3f,j). Given hydrogenotrophic methanogenesis as the dominant  $CO_2$  uptake process, we estimate that  $CO_2$  production would have to be at least 5–10 $\times$  higher in continuously anoxic peats (e.g., reaching 5,000–10,000 ppmv) to achieve the methane yields



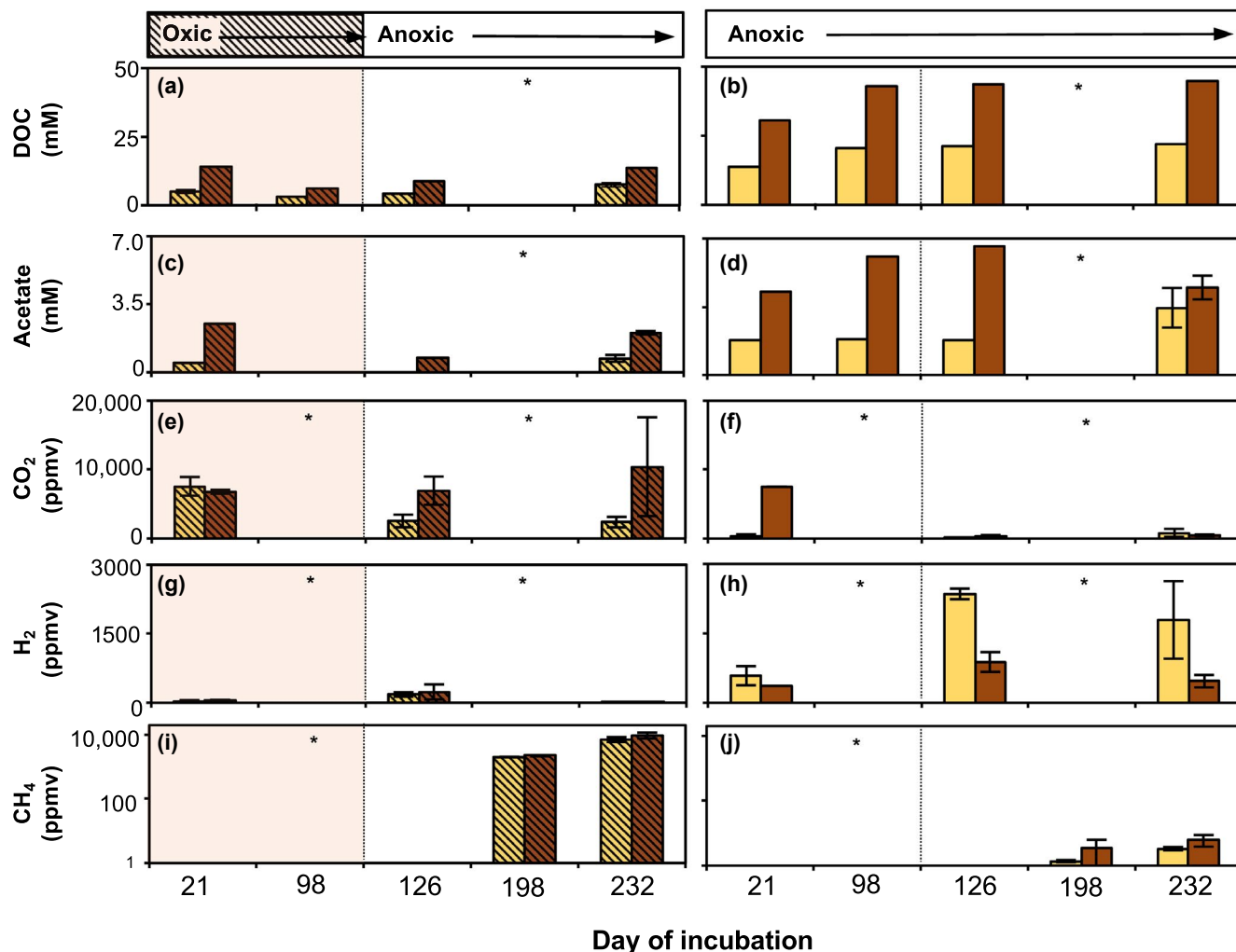


**FIGURE 3** Effect of  $O_2$  on peat chemistry across an oxic-anoxic transition. (a–j) Aqueous (DOC, dissolved organic carbon) and gas phase chemistry of moderately (AWT layer, light orange bars) and highly degraded (BWT layer, brown bars) peats exposed to 5%  $O_2$  followed by incubation under anoxic conditions (hatched bars, left panels) or kept continuously anoxic (solid bars, right panels). Incubations of a given peat layer under redox-oscillated or continuously anoxic conditions were initiated with the same batch of peat slurry (see Section 2). Vertical dotted lines denote the transition between incubation with headspace flushing and without headspace exchange. Asterisk symbols (\*) indicate days for which data are unavailable. Error bars represent the standard error of  $n = 2$  or 3 biological replicates. Data for other layers and 10%  $O_2$ -treated peat are in Figure S2

of redox-oscillated peat. Higher concentrations of organic acids in the acidic, continuously anoxic peats (Figure 3d; Figure S2) may have further limited methanogenesis (Field & Lettinga, 1987, 1992; Horn et al., 2003; Patra & Saxena, 2010).

In contrast to chemical indications of hydrogenotrophic methanogenesis, we found little evidence for  $CH_4$  generated by the acetoclastic pathway. As expected, acetate concentrations (Figure 3c,d; Figure S2) in peat slurries were much lower during  $O_2$  treatment than during anoxic periods due to aerobic heterotrophic consumption of an initial acetate pool and  $O_2$  inhibition of anaerobic fermentation. Under anoxic conditions, when acetoclastic methanogenesis is expected to limit acetate accumulation, we instead observed increasing acetate concentrations, with continuously anoxic peats exhibiting much higher concentrations (~2 to 5 $\times$ ) than  $O_2$ -treated samples by the end of the incubation. Similar trends were observed

for levels of propionate and butyrate, which are other typical fermentation products (Figure S2). The association of the greatest levels of acetate buildup with the lowest  $CH_4$  yields at the end of the incubation period in continuously anoxic controls (Figure 3d,j) is similar to observations in long-term slurry incubations from other *Sphagnum*-dominated peatlands, where acetate, rather than  $CH_4$ , was the dominant end product of anaerobic metabolism (Hines et al., 2008). The notable absence of acetoclastic methanogenesis could reflect the toxicity of plant tannins and other aromatic structures to methanogens (Field & Lettinga, 1987, 1992; Patra & Saxena, 2010) or result from the acidic pH of slurries (pH ~4.0), as the accumulation of free acetic acid ( $pK_a$  4.75) can decouple membrane potential (Bräuer et al., 2004; Horn et al., 2003).

To better understand changes in peat chemical composition over the course of incubation, we analyzed the DOC from 5%  $O_2$ -treated

and continuously anoxic AWT and BWT peat slurry samples using high-resolution mass spectrometry (FT-ICR-MS). This method characterizes molecules between 200 and 1200  $m/z$  with parts-per-million mass accuracy. To assess broad-scale variations in the molecular diversity of DOC, we first analyzed the data based on the presence/absence detection of unique molecular formulae (i.e., multiple detections of an individual molecule were excluded, Figure 4, Table S1). The most notable differences between  $O_2$ -treated and continuously anoxic control samples occurred near the redox transition and at the end of the incubation when comparing the average exact mass, NOSC, AI, and DBE/C of unique molecules detected within peat DOC from each layer (Figure 4; Table S2). For both  $O_2$ -treated and fully anoxic peats, the average exact mass of unique DOC molecules increased from *ca* 500–507 Da at day 21 to *ca* 520–550 Da over the first 98 days of incubation (i.e., prior to the redox switch in oxygenated samples), but then decreased to *ca* 484–497 Da by the end of the experiment at day 232. Average exact masses at a given time point varied up to 10% based on oxygen treatment and

on peat layer type. The average values of NOSC, DBE/C, and AI of unique compounds in  $O_2$ -treated and continuously anoxic samples increased during the first 98 days of incubation, with no obvious difference in changes based on treatment. However, NOSC, DBE/C, and AI were all larger for  $O_2$ -exposed samples compared to anoxic controls by the end of the experiment. Taken together, DOC compound diversity measurements suggest that (1) larger molecules, on average, are processed to smaller molecules over months-long periods regardless of redox transition in a closed system, and (2) prior oxygenation increases the oxidation state, double bond, and aromaticity characteristics of peat C during downstream anaerobic processing.

We then assessed DOC diversity across major molecular classes (lipids, proteins, amino sugars, carbohydrates, lignins, tannins, condensed aromatics, unsaturated hydrocarbons) using the ratios of O/C, H/C, N/C, and the AI value of individual unique formulae (Table S1). Lignin-like molecules were the dominant forms of uniquely detected DOC (~60%–70% formulae), followed by tannin-like

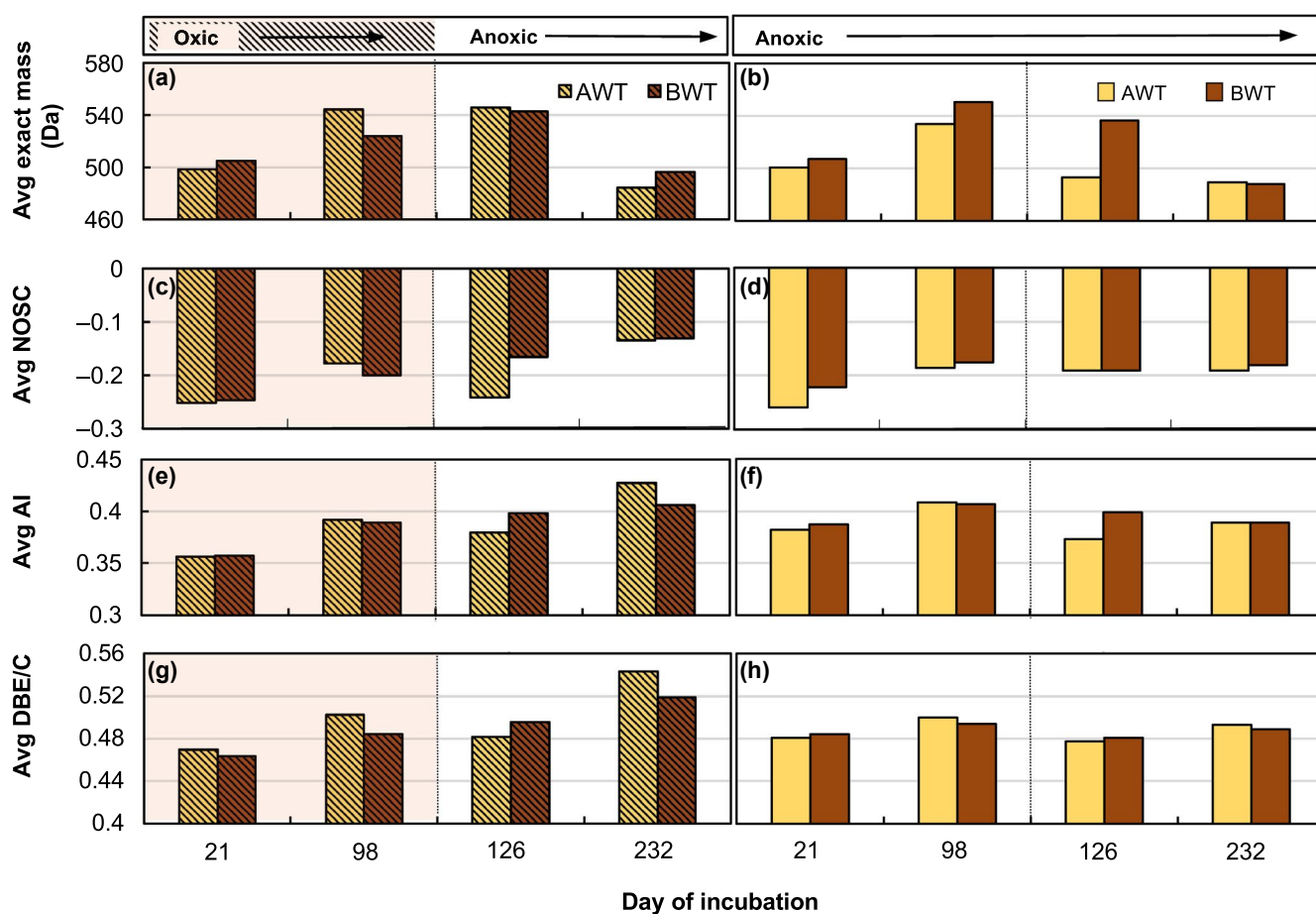


**FIGURE 4** Effect of  $O_2$  on the average exact mass, nominal oxidation state (NOSC), double bond equivalency (DBE/C), and aromaticity index (AI) of unique DOC molecules detected by FT-ICR-MS (a–h). Results from moderately (AWT; light orange bar) and highly degraded (BWT; brown bar) peat slurries exposed to 5%  $O_2$  followed by incubation under anoxic conditions (left panels) or kept continuously anoxic (right panels). Vertical dotted line denotes the transition between incubation with headspace flushing and without headspace exchange. Each bar represents the FT-ICR-MS results of an individual sample. Averages are based solely on the diversity of unique molecules detected by FT-ICR-MS

compounds (~10%–20%). Condensed aromatics (~5%–15%), carbohydrates (0%–5%), peptide and amino sugars (0%–5%), lipids (<3%), and unsaturated hydrocarbons (<3%) were relatively minor contributors to detected DOC diversity. We found overlapping distributions of molecules among the various molecular classes in samples that were O<sub>2</sub> treated, continuously anoxic, and from different peat layers (Table S1, % Formulae column). The absence of obvious differences in DOC molecular class diversity prompted us to analyze the FT-ICR-MS data based on the relative abundance of detected molecules (Figure 5) as has been performed in other studies investigating relative compositional changes in similar sample types (Naughton et al., 2021; Wozniak et al., 2020).

A PCA of FT-ICR-MS data strongly support the importance of oxygenation and incubation time in shaping DOC composition. The distinct sample groupings based on O<sub>2</sub> treatment and time in the PCAs (Figure 5a,b) indicate that DOC composition varies based on these incubation parameters. The largest changes in DOC composition occurred over several months, becoming most apparent between O<sub>2</sub>-treated samples and anoxic controls by the end of the experiment at 232 days (Figure 5a,b). In contrast, DOC composition could not be distinguished based on peat layer type (Figure 5c), likely because both layers contained a large amount of degraded plant material (Figure 2a). To better understand specific differences in the molecular composition of the DOC pool between samples, we identified individual compounds that increased with time or with oxygenation based on their PCA axes loadings at the end of the incubation when differences in DOC composition were greatest (Figure 5a,b; Figure S4). While Van Krevelen diagrams (Figure 5d,e) indicate that affected molecules span all molecular classes, O<sub>2</sub> treatment led to a prominent enrichment of certain compounds with lower H/C (~0.5–1.0) and higher O/C ratios (~0.4–0.7) within the condensed aromatic-, lignin-, and tannin-like molecular classes. Less obvious enrichments of a higher H/C (~1.5) subgroup of lignin-like molecules and lower O/C (~0.2) condensed aromatics were also observed. In contrast to the O<sub>2</sub>-treated samples, continuously anoxic samples were predominantly enriched with certain higher H/C (~1–1.75) and lower O/C ratios (~0.2–0.4) lignin-like molecules, as well as lipid- and protein-like compounds. In support of the Van Krevelen data, we found that the NOSC, DBE/C, and AI values for many molecules increased with O<sub>2</sub> pretreatment relative to anoxic controls by the end of the incubation (Figure S4).

The distinctive enrichment of more oxidized, double-bonded, aromatic molecules, many falling into the condensed aromatics molecular class (Figure 5; Figure S4), within redox-oscillated peat likely reflects greater microbial processing of certain lignin- and tannin-like molecules that is enabled by transient O<sub>2</sub> exposure (Figure 1). It is also possible that the oxidative exposure of the peat could promote abiotic Fenton-like oxidation which has been shown to lead to increased levels of oxidized lignin molecules that plot on van Krevelen diagrams as condensed aromatics or tannin-like molecules (Waggoner et al., 2017). In line with this microbial interpretation, an FT-ICR-MS study of DOM across the depth of a peat column documented a buildup of condensed aromatics in peat undergoing the

greatest redox oscillation and suggested a likely biotic origin to such compounds (Tfaily et al., 2018). In the continuously anoxic peats, the enrichment of diverse reduced forms of lignin-like molecules, which have relatively high H/C and low O/C, along with certain proteins and lipids (Figure 5d,e) points to more limited use of highly reduced C molecules as food and energy sources by the microbial community. This is likely due to the absence of a strong oxidant as well as biochemical constraints on C degradation imposed by anoxic limitation of aromatic oxygenase activity. In line with our findings, a recent study observed an increase in the relative abundance of lignin-like structures with soil anoxia, attributing such results to oxygen inhibition of oxidative enzymes (Naughton et al., 2021). Increases in lipid/protein-rich DOC have been observed in anaerobic incubations of aquifer sediment organic matter, likely due to the slower turnover of these microbially derived compounds resulting from thermodynamic barriers to microbial metabolism of low NOSC in highly reduced systems (Pracht et al., 2018). In agreement with compound-specific indications of lower peat C bioavailability in the absence of O<sub>2</sub>, we measured higher levels of DOC in continuously anoxic peat samples (Figure 3).

Collectively, DOC characterization shows that while redox oscillation leads to considerably reduced total DOC levels, the effect does not generally lead to discernable changes in overall C distribution across the main molecular classes, aside from the condensed aromatics (Figure 5; Table S1; Figure S3). Rather, the data suggest the importance of tracking changes in specific lignin- and tannin-like molecules to ascertain biogeochemical pathways of C flow using gene-based assessments on microbial C transformation mechanisms along with stable isotope tracing of those compounds. Compound-specific approaches are also supported by findings of variable biogeochemical activity across different forms of phenolic compounds (Adamczyk et al., 2017; Zak et al., 2019).

### 3.3 | O<sub>2</sub> directs microbial function across the redox transition to promote anaerobic CH<sub>4</sub> production

To elucidate the microbial composition and functions in peat slurries, we performed DNA sequencing of 16S rRNA gene amplicons and peat microbial metagenomes. Broad comparisons of 16S rRNA gene amplicon and metagenomic sequence data from peat slurries indicate that the greatest variations in the peat microbiome were associated with O<sub>2</sub> treatment (Figures S6 and S7). The most striking differences between O<sub>2</sub>-treated and continuously anoxic peat metagenomes involve genes related to aromatic C degradation (Figures S6 and S7). We observed large increases in 16S amplicon (up to ~80% amplicons, Figure 6a) and metagenomic sequences (up to ~40% of all reads, Figure S5) for *Novosphingobium*, a bacterial genus in *Sphagnum* mosses (Bragina et al., 2012). Importantly, this genus has been characterized by its versatile O<sub>2</sub>-dependent metabolism of aromatic compounds and resistance to xenobiotics in other natural and synthetic systems (Kumar et al., 2017; Tiirola et al., 2002). We hypothesize that these unique functional capabilities

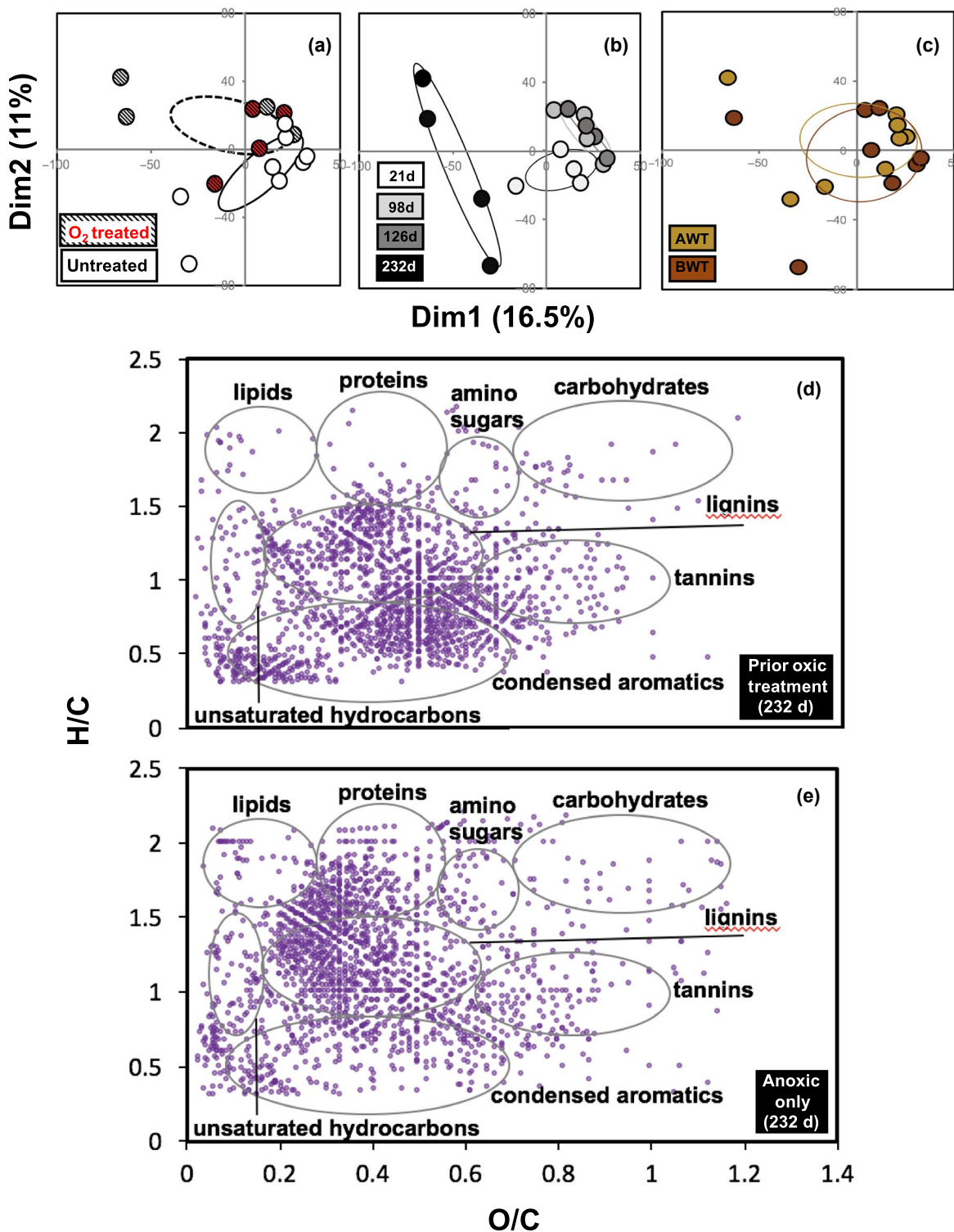
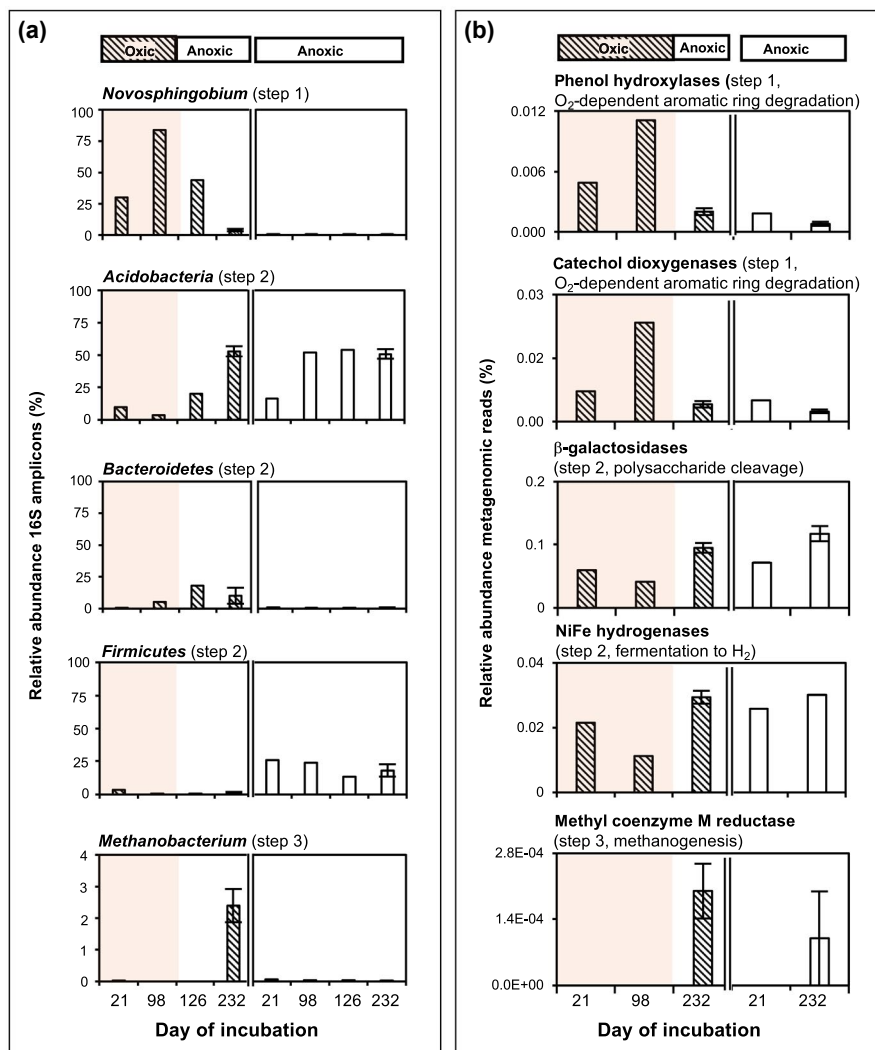


**FIGURE 5** Principal component analysis (PCA) of peat DOC based on FT-ICR-MS relative intensities of all detected compounds from O<sub>2</sub>-treated and continuously anoxic incubations of AWT and BWT peat layers. (a–c) Centroids, enclosed by 95% confidence ellipses, of the data analyzed by O<sub>2</sub> treatment (a), incubation time (b), and peat layer (c) show the influence of O<sub>2</sub> treatment and incubation time on DOC molecular composition. (d) Van Krevelen diagram of DOC molecules from AWT and BWT peat that were most strongly influenced (increased in relative abundance) by the end of incubation at 232 days and by prior oxically treatment (i.e., molecules with negative loadings on PC1, positive loadings on PC2). (e) Van Krevelen diagram of DOC molecules from AWT and BWT peat that were most strongly influenced (increased) by time at 232 days and continuous anoxic treatment (i.e., molecules with negative loadings on PC1, negative loadings on PC2). Gray circles depict regions of H/C and O/C characteristics of various molecular classes

**FIGURE 6** Effect of O<sub>2</sub> exposure on peat microbiology across an oxic–anoxic redox transition (a) Relative abundance of key microbial groups inferred from 16S rRNA gene amplicon sequencing of 5% O<sub>2</sub>-treated and continuously anoxic peats. Step numbers refer to the degradation scheme presented in Figure 1.

(b) Relative abundance of select metagenomic functional genes in 5% O<sub>2</sub>-treated and continuously anoxic peats. Red shading indicate time points under oxygenation treatment. Bars for time points before day 232 comprise sequences from DNA extractions of pooled layers. Standard error bars (day 232) were calculated by pooling layer specific data (duplicate 16S datasets for UNS, AWT, and BWT layers; duplicate metagenome datasets for UNS, AWT, and BWT layers for O<sub>2</sub>-treated peats; a single UNS and BWT layer metagenome for continuously anoxic peats)



may be particularly important for allowing *Novosphingobium* to withstand or mitigate any potential toxicity brought on by peat polyphenols during degradation of organic C. In contrast to findings for oxygenated samples, *Novosphingobium* 16S amplicon and metagenomic sequences remained conspicuously low in continuously anoxic peats (<1% of amplicon and metagenomic sequences, Figure 6a; Figure S5).

Consistent with 16S amplicon data, metagenomic sequences for phenol hydroxylases and catechol dioxygenases (aromatic oxygenases that degrade aromatic rings using O<sub>2</sub> as a co-substrate (Harayama et al., 1992)) rose during O<sub>2</sub> treatment (Figure 6b). They reached their highest relative abundances by the end of the oxic phase, when ~50%–90% of metagenomic reads most closely matched those in *Novosphingobium* (Table S5). During the subsequent anoxic incubation phase, aromatic oxygenase sequences decreased in relative abundance to levels similar to those in continuously anoxic peats (Figure 6b). The importance of aromatic metabolism in aerobic C degradation is also demonstrated by the higher relative abundance of sequences for all forms of aromatic metabolism during O<sub>2</sub> treatment compared to anoxic conditions (Figure S8). Our results suggest that *Novosphingobium* could taxonomically and genetically serve as

a unique biomarker in the field, at least in certain peatlands, to help predict how oxygenation might trigger degradation of complex OC and potentially fuel CH<sub>4</sub> production. Theoretically, the presence of *Novosphingobium* genomes, not just individual oxidase genes, could greatly improve the delineation and modeling of redox transition zones in peatlands that are vulnerable to climate change.

Sequence data suggest a central role for *Acidobacteria* in anaerobic C processing of peats (Figure 1, step 2; Figure 6a). The *Acidobacteria* are a poorly understood phylum of heterotrophic bacteria found in soil environments (Dedysh et al., 2006; Kielak et al., 2016). These organisms generally account for a large fraction of the microbial community under anoxic conditions in our experiment (Figure 6a; Figures S4 and S5) and encode the greatest proportion of  $\beta$ -galactosidase (a common glycoside hydrolase involved in polysaccharide degradation) and NiFe hydrogenase sequences (involved in fermentative H<sub>2</sub> production) that can be taxonomically identified within metagenomes (Table S5). Overall, the relative abundance of genes for  $\beta$ -galactosidase and NiFe hydrogenase were similar in anoxic phase metagenomes regardless of O<sub>2</sub> treatment (Figure 6b).

There was a marked increase in the relative abundance of 16S rRNA gene sequences of *Holophaga* (a genus of *Acidobacteria*)

following the redox transition compared to strictly anoxic controls (Figure S6). Notably, anaerobic bacteria belonging to *Holophaga* are able to degrade methoxylated aromatics and are capable of producing CO<sub>2</sub> (an important substrate for hydrogenotrophic methanogenesis) in the initial decarboxylation step of aromatic degradation (Anderson et al., 2012). A possible explanation for why *Holophaga* remained lower in relative abundance in the anoxic control samples compared to O<sub>2</sub> treatments following the redox transition is that the DOC of anoxic control samples was lacking in methoxylated derivatives produced by microbes like *Novosphingobium* to serve as substrates for *Holophaga*. Accordingly, recent LC/MS characterizations (Ohta et al., 2015) have shown that incubation of *Novosphingobium* with wood-derived, lignin-like, extracts leads to the generation of methoxylated metabolites and other depolymerization by-products of lignin and lignin-like compounds (Figure S3; Table S1). This helps explain the increased degradation and mineralization of OC during anaerobic conditions following the redox transition in our study, considering that oxygenation led to high relative abundances of *Novosphingobium* (a putative methoxylated-aromatic producer) and *Holophaga* (a putative methoxylated-aromatic consumer) before and after the redox transition, respectively. Our data suggest that members of these two genera could provide a specialized microbial pathway for the efficient degradation of polyphenolic substrates under oxygen variable conditions, which could ultimately lead to increased CH<sub>4</sub> emissions.

The taxonomic analyses of 16S amplicons (Figure 6a; Figure S4) and metagenomes (Table S5) additionally suggest the importance of *Proteobacteria*, *Bacteroidetes*, and *Firmicutes* for the anoxic decomposition of peat leading to the production of fermentation end products such as acetate, propionate, H<sub>2</sub>, and CO<sub>2</sub>. In both O<sub>2</sub>-treated and anoxic control samples, we identified sequences from the genus *Thermacetogenium*, a *Firmicutes* genus that is known to syntrophically couple anaerobic acetate oxidation to hydrogenotrophic methanogenesis (Hattori et al., 2000), making it possible that some acetate produced in our incubations had the potential to be converted to CH<sub>4</sub> through a cryptic syntrophic pathway. Additionally, many of the fermenting microbes (e.g., *Clostridium* sp.) detected in our study have some potential of fixing CO<sub>2</sub> and H<sub>2</sub>. Thus, future studies that seek to unravel the biogeochemistry of redox-dynamic peats should account for these poorly characterized pathways, possibly by applying stable isotope probes (SIP) to obtain more precise accounting of the microbes driving the involved C flows.

The 16S rRNA gene sequencing data indicate that *Methanobacterium* was likely the primary methanogen in the peat driving CH<sub>4</sub> production by the end of the experiment (Figure 6). This is important because hydrogenotrophic *Methanobacterium* species use the reduction of CO<sub>2</sub> with H<sub>2</sub> during the production of CH<sub>4</sub> (Galand et al., 2005; Kotsyurbenko et al., 2007). The predominance of *Methanobacterium* is also consistent with the low pH (pH range 3.7–4.2) of the peat during our experiment. Previous studies have shown that *Methanobacterium* grows in acidic peats and is capable of living under extremes of pH (pH = 3–9; Galand et al., 2005; Kotsyurbenko et al., 2007). Furthermore, we observed a larger relative abundance

of 16S rRNA gene sequences for *Methanobacterium* than for other methanogenic genera at every time point sampled for DNA during the incubation (Table S2). Consistent with higher CH<sub>4</sub> yields from peat slurries after O<sub>2</sub> treatment (Figure 2; Figure S1), as well as the 16S amplicon (Figure 6a) and metagenomic data (Figure 6b; Table S5), the analysis of the methanogenesis biomarker gene, methyl coenzyme M reductase (*mcrA*, Figure S9), indicated a larger contribution of methanogens to anoxic phase microbiomes of O<sub>2</sub>-treated peats compared to continuously anoxic peats. Importantly, over >99.9% of methanogen 16S amplicon and *mcrA* sequences in peats (Tables S2 and S5) match those of *Methanobacterium* (Kotsyurbenko et al., 2007; Morgan et al., 1997). The conspicuous absence of 16S and *mcrA* gene sequences for acetoclastic methanogens in our dataset has also been observed in other *Sphagnum*-dominated peatlands (Rooney-Varga et al., 2007), including one site in a temperate wetland, close to where this peat was collected.

### 3.4 | Possible abiotic C degradation in peat

Abiotic processes based on the co-occurrence of solid-phase Fe(II) species and O<sub>2</sub> can lead to Fenton-like (i.e., heterogeneous Fenton) reactions that generate hydroxyl radicals to oxidize soil OC (Page et al., 2013; Trusiak et al., 2018; Waggoner et al., 2017), supplementing biotic OC mineralization. Recent studies have shown that Fe solid phases (e.g., Fe(II)/Fe(III) nano-magnetite and solid-phase Fe(II) at the surface of reactive Fe-(oxyhydr)oxides like ferrihydrite and goethite) undergo Fenton catalysis and facilitate the oxidation of natural OC (Chen et al., 2021; Rose & Waite, 2003). Consequently, the presence of Fe(II)/Fe(III) solid phases are critical indicators of OC degradation in redox-dynamic environments. To explore the possibility of abiotic C degradation catalyzed by heterogeneous Fenton reactions in our incubations, we performed X-ray analyses (XANES) of solid-phase Fe chemical speciation in peat (Figure 7). Fe(II) species were substantially present even during oxygenation of the peat based on the relative proportions of Fe(III) and Fe(II) (Figure 7), findings consistent with the analyses of redox-stratified peatlands (Bhattacharyya et al., 2018). Such data support the potential for abiotic C degradation in laboratory redox-oscillated peat. More targeted experiments that distinguish abiotic and biotic transformations are needed to understand how abiotic reactions affect peat C composition and methanogenesis. In particular, the coupling of abiotic processes to biotic processes that fuel downstream methanogenesis is not known. Continued future work is therefore warranted to investigate the role of abiotic mechanisms in regulating methanogenesis following redox transitions in peatlands.

### 3.5 | Field extrapolations

We note that the results determined from “bottle” incubations, as were used here and in other studies (e.g., Brouns et al., 2014), are difficult to extrapolate to the field due to a variety of potential artifacts

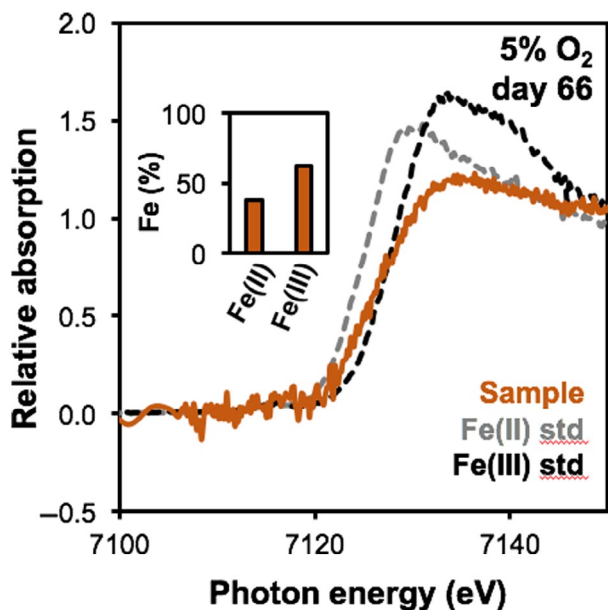


**FIGURE 7** Iron redox state in peat during oxygenation treatment. XANES analyses of Fe redox state in representative solid-phase Fe hotspots within pooled layers of 5% O<sub>2</sub>-treated peat during the oxic phase of incubation at day 66

imposed by methodology that may have opposing effects on CH<sub>4</sub> production. For example, blending of the peat matrix into a slurry could lead to cell lysis of a portion of the microbial population, including the methanogens; peat homogenization could also alter the abundance and composition of soluble C substrates available for downstream methanogenesis. Although these microbial and chemical effects from initially blending the peat most likely occurred, our results, which derive from comparisons of temporal changes in geochemistry and microbiology in the same initial batch of peat slurry subject to varying O<sub>2</sub> treatment, conclusively show that oxygenation increases CH<sub>4</sub> production during a subsequent anoxic period. The concepts, organic C transformations, and microbial gene signatures on the mechanism of O<sub>2</sub>-enhanced methanogenesis outlined from our laboratory study can inform further laboratory and field research that explores the role of redox-oscillation timing, soil chemistry, and microbiology in controlling CH<sub>4</sub> emissions across different wetland types.

## 4 | CONCLUSIONS

Using coupled analyses of peat geochemistry and microbiology, we demonstrate that striking enhancements of peat CH<sub>4</sub> yield after O<sub>2</sub> exposure result from specific changes in microbial community diversity and function that are shaped by C chemistry and O<sub>2</sub>. The data can help explain field observations of major CH<sub>4</sub> emissions from soils and peats exposed to O<sub>2</sub> (e.g., Angle et al., 2017; Shoemaker et al., 2012; Yang et al., 2017). Sequencing results are wholly consistent with our chemical data, confirming H<sub>2</sub> and CO<sub>2</sub> as critical pathway

intermediates for O<sub>2</sub>-enhanced CH<sub>4</sub> production by *Sphagnum* peat. Importantly, the combined chemical and sequence data indicate the “gatekeeping” role of specific microbes like *Novosphingobium* which encode oxidase enzymes that can efficiently degrade complex peat C during the oxic period, and thus promote subsequent anoxic phase C flow toward CH<sub>4</sub> production by hydrogenotrophic methanogens. Our data support a holistic view of soil C storage and transformation that incorporates information on environmental conditions (e.g., O<sub>2</sub>, water table), molecular form, and microbial biodiversity, with a strong focus on the interplay of these factors.

Our data, which help explain field observations of large CH<sub>4</sub> emissions from certain soils and peats exposed to O<sub>2</sub> (Angle et al., 2017; Longhi et al., 2016; O’Connell et al., 2018; Shoemaker & Schrag, 2010; Shoemaker et al., 2012; Teh et al., 2005; Turetsky et al., 2014; Yang et al., 2017), point to the critical role of microbial dynamics across spatial or temporal transitions between oxic and anoxic conditions in determining wetland CH<sub>4</sub> emissions. Indeed, increased greenhouse gas emissions following redox transitions, typically modulated by hydrology, have been observed for soils after drought recovery (O’Connell et al., 2018) and for drained wetlands after their restoration (Abdalla et al., 2016). The mechanistic findings of our study imply that an improved understanding of wetland microbiomes in redox-dynamic settings may help constrain methane budgets. They also highlight the potential for positive climate feedback between hydrologic variability and CH<sub>4</sub> emissions from wetlands, particularly in tropical and high latitude regions where climate change is altering hydrology by shifting rainfall patterns (Chadwick et al., 2015; Dean et al., 2018) or promoting rapid permafrost thaw (Hodgkins et al., 2014). It follows that strategies to limit CH<sub>4</sub> emissions from natural and constructed wetlands, as part of land-based climate solution initiatives, should focus on water management in order to account for the ways in which water availability shapes spatiotemporal transitions in O<sub>2</sub> concentration and affects CH<sub>4</sub> production.

## ACKNOWLEDGMENTS

The authors thank X. Liao and the late M. Hines for aid in sample collection; S. Haynes, G. D’Arcangelo, A. Maloney, and A. Goranov for experimental and data analysis support; F. Morel, F. Paulot, and S. Myneni for project discussions. This study was supported by the Carbon Mitigation Initiative at Princeton University; National Science Foundation Graduate Research Fellowship under Grant No. DGE 1842213 (to S.W.R.); National Science Foundation Award CHE-1610021 (to P.G.H.); GeoSoilEnviroCARS (Sector 13), which is funded by the National Science Foundation - Earth Sciences (EAR-1128799); and the Department of Energy, Geosciences (DE-FG02-94ER14466). This research used beamline 5-ID (SRX) of the National Synchrotron Light Source II, a US Department of Energy (DOE) Office of Science User Facility operated for the DOE Office of Science by Brookhaven National Laboratory under Contract No. DE-SC0012704, and resources of the Advanced Photon Source, a U.S. Department of Energy (DOE) Office of Science User Facility operated for the DOE Office of Science by Argonne National Laboratory under Contract No. DE-AC02-06CH11357.

## CONFLICT OF INTEREST

The authors declare no competing interests.

## AUTHOR CONTRIBUTIONS

X. Zhang, J. K. Schaefer, and J. K. Shoemaker conceived of the study and carried out fieldwork. J. L. Wilmoth, J. K. Schaefer, and X. Zhang performed incubation experiments. J. L. Wilmoth, J. K. Schaefer, D. R. Schlesinger, P. G. Hatcher, and X. Zhang performed chemical analyses; J. L. Wilmoth, S. W. Roth, and J. K. Schaefer performed the bioinformatic analyses. J. L. Wilmoth and X. Zhang wrote the first draft of the manuscript; all authors contributed to interpretation of the results and edited the manuscript.

## DATA AVAILABILITY STATEMENT

Sequence data have been deposited at NCBI under SRA accession PRJNA551662. All other data are available in the Supplementary files and by request from the authors.

## ORCID

Jeffra K. Schaefer  <https://orcid.org/0000-0002-9916-8078>

Danielle R. Schlesinger  <https://orcid.org/0000-0002-0757-9209>

Spencer W. Roth  <https://orcid.org/0000-0001-9559-1154>

Xinning Zhang  <https://orcid.org/0000-0003-2763-1526>

## REFERENCES

- Abdalla, M., Hastings, A., Truu, J., Espenberg, M., Mander, U., & Smith, P. (2016). Emissions of methane from northern peatlands: A review of management impacts and implications for future management options. *Ecology and Evolution*, 6(19), 7080–7102. <https://doi.org/10.1002/ece3.2469>
- Adamczyk, B., Karonen, M., Adamczyk, S., Engström, M. T., Laakso, T., Saranpää, P., Kitunen, V., Smolander, A., & Simon, J. (2017). Tannins can slow-down but also speed-up soil enzymatic activity in boreal forest. *Soil Biology and Biochemistry*, 107, 60–67. <https://doi.org/10.1016/j.soilbio.2016.12.027>
- Amir, A., McDonald, D., Navas-Molina, J. A., Kopylova, E., Morton, J. T., Zech Xu, Z., Kightley, E. P., Thompson, L. R., Hyde, E. R., Gonzalez, A., & Knight, R. (2017). Deblur rapidly resolves single-nucleotide community sequence patterns. *mSystems*, 2(2), e00191–e1116. <https://doi.org/10.1128/mSystems.00191-16>
- Anderson, I., Held, B., Lapidus, A., Nolan, M., Lucas, S., Tice, H., Del Rio, T. G., Cheng, J.-F., Han, C., Tapia, R., Goodwin, L. A., Pitluck, S., Liolios, K., Mavromatis, K., Pagani, I., Ivanova, N., Mikhailova, N., Pati, A., Chen, A., ... Kyrpides, N. C. (2012). Genome sequence of the homoacetogenic bacterium *Holophaga foetida* type strain (TMBS4(T)). *Standards in Genomic Sciences*, 6(2), 174–184. <https://doi.org/10.4056/signs.2746047>
- Angle, J. C., Morin, T. H., Solden, L. M., Narrowe, A. B., Smith, G. J., Borton, M. A., Rey-Sanchez, C., Daly, R. A., Mirfenderesgi, G., Hoyt, D. W., Riley, W. J., Miller, C. S., Bohrer, G., & Wrighton, K. C. (2017). Methanogenesis in oxygenated soils is a substantial fraction of wetland methane emissions. *Nature Communications*, 8(1), 1567. <https://doi.org/10.1038/s41467-017-01753-4>
- Bengtsson, F., Rydin, H., & Hájek, T. (2018). Biochemical determinants of litter quality in 15 species of Sphagnum. *Plant and Soil*, 425, 161–176. <https://doi.org/10.1007/s11104-018-3579-8>
- Bhat, T. K., Singh, B., & Sharma, O. P. (1998). Microbial degradation of tannins – A current perspective. *Biodegradation*, 9(5), 343–357. <https://doi.org/10.1023/A:1008397506963>
- Bhattacharyya, A., Schmidt, M. P., Stavitski, E., & Martínez, C. E. (2018). Iron speciation in peats: Chemical and spectroscopic evidence for the co-occurrence of ferric and ferrous iron in organic complexes and mineral precipitates. *Organic Geochemistry*, 115, 124–137. <https://doi.org/10.1016/j.orggeochem.2017.10.012>
- Bolger, A. M., Lohse, M., & Usadel, B. (2014). Trimmomatic: A flexible trimmer for Illumina sequence data. *Bioinformatics*, 30(15), 2114–2120. <https://doi.org/10.1093/bioinformatics/btu170>
- Bragina, A., Berg, C., Cardinale, M., Scherbakov, A., Chebotar, V., & Berg, G. (2012). Sphagnum mosses harbour highly specific bacterial diversity during their whole lifecycle. *The ISME Journal*, 6(4), 802–813. <https://doi.org/10.1038/ismej.2011.151>
- Bräuer, S. L., Yavitt, J. B., & Zinder, S. H. (2004). Methanogenesis in McLean bog, an acidic peat bog in upstate New York: stimulation by H<sub>2</sub>/CO<sub>2</sub> in the presence of rifampicin, or by low concentrations of acetate. *Geomicrobiology Journal*, 21(7), 433–443. <https://doi.org/10.1080/01490450490505400>
- Brouns, K., Verhoeven, J. T. A., & Hefting, M. M. (2014). Short period of oxygenation releases latch on peat decomposition. *Science of the Total Environment*, 481, 61–68. <https://doi.org/10.1016/j.scitotenv.2014.02.030>
- Brown, J., Pirrung, M., & McCue, L. A. (2017). FQC Dashboard: Integrates FastQC results into a web-based, interactive, and extensible FASTQ quality control tool. *Bioinformatics*, 33(19), 3137–3139. <https://doi.org/10.1093/bioinformatics/btx373>
- Buchfink, B., Xie, C., & Huson, D. H. (2015). Fast and sensitive protein alignment using DIAMOND. *Nature Methods*, 12(1), 59–60. <https://doi.org/10.1038/nmeth.3176>
- Caporaso, J. G., Kuczynski, J., Stombaugh, J., Bittinger, K., Bushman, F. D., Costello, E. K., Fierer, N., Peña, A. G., Goodrich, J. K., Gordon, J. I., Huttley, G. A., Kelley, S. T., Knights, D., Koenig, J. E., Ley, R. E., Lozupone, C. A., McDonald, D., Muegge, B. D., Pirrung, M., ... Knight, R. (2010). QIIME allows analysis of high-throughput community sequencing data. *Nature Methods*, 7(5), 335–336. <https://doi.org/10.1038/nmeth.f.303>
- Chadwick, R., Good, P., Martin, G., & Rowell, D. P. (2015). Large rainfall changes consistently projected over substantial areas of tropical land. *Nature Climate Change*, 6, 177. <https://doi.org/10.1038/nclimate2805>
- Chen, Y., Miller, C. J., & Waite, T. D. (2021). Heterogeneous fenton chemistry revisited: mechanistic insights from ferrihydrite-mediated oxidation of formate and oxalate. *Environmental Science & Technology*. <https://doi.org/10.1021/acs.est.1c00284>
- Clymo, R. S., Pearce, D. M. E., Conrad, R., Fowler, D., Jenkinson David, S., Monteith John, L., & Unsworth, M. H. (1995). Methane and carbon dioxide production in, transport through, and efflux from a peatland. *Philosophical Transactions of the Royal Society of London Series A: Physical and Engineering Sciences*, 351(1696), 249–259. <https://doi.org/10.1098/rsta.1995.0032>
- Dean, J. F., Middelburg, J. J., Röckmann, T., Aerts, R., Blauw, L. G., Egger, M., Jetten, M. S. M., de Jong, A. E. E., Meisel, O. H., Rasigraf, O., Slomp, C. P., in't Zandt, M. H., & Dolman, A. J. (2018). Methane feedbacks to the global climate system in a warmer world. *Reviews of Geophysics*, 56(1), 207–250. <https://doi.org/10.1002/2017R000559>
- Dedysh, S. N., Pankratov, T. A., Belova, S. E., Kulichevskaya, I. S., & Liesack, W. (2006). Phylogenetic analysis and in situ identification of bacteria community composition in an acidic sphagnum peat bog. *Applied and Environmental Microbiology*, 72(3), 2110. <https://doi.org/10.1128/AEM.72.3.2110-2117.2006>
- DiDonato, N., Chen, H., Waggoner, D., & Hatcher, P. G. (2016). Potential origin and formation of molecular components of humic acids in soils. *Geochimica et Cosmochimica Acta*, 178, 210–222. <https://doi.org/10.1016/j.gca.2016.01.013>
- Duddleston, K. N., Kinney, M. A., Kiene, R. P., & Hines, M. E. (2002). Anaerobic microbial biogeochemistry in a northern bog: Acetate



- as a dominant metabolic end product. *Global Biogeochemical Cycles*, 16(4), 11–11–11–19. <https://doi.org/10.1029/2001GB001402>
- Fan, Z., Neff, J. C., Waldrop, M. P., Ballantyne, A. P., & Turetsky, M. R. (2014). Transport of oxygen in soil pore-water systems: Implications for modeling emissions of carbon dioxide and methane from peatlands. *Biogeochemistry*, 121, 455–470. <https://doi.org/10.1007/s10533-014-0012-0>
- Fenner, N., & Freeman, C. (2011). Drought-induced carbon loss in peatlands. *Nature Geoscience*, 4, 895. <https://doi.org/10.1038/ngeo1323>
- Field, J. A., & Lettinga, G. (1987). The methanogenic toxicity and anaerobic degradability of a hydrolyzable tannin. *Water Research*, 21(3), 367–374. [https://doi.org/10.1016/0043-1354\(87\)90217-X](https://doi.org/10.1016/0043-1354(87)90217-X)
- Field, J. A., & Lettinga, G. (1992). Toxicity of tannic compounds to microorganisms. In R. W. Hemingway & P. E. Laks (Eds.), *Plant polyphenols: Synthesis, properties, significance* (Vol. 59, pp. 673–692). Springer US. [https://doi.org/10.1007/978-1-4615-3476-1\\_39](https://doi.org/10.1007/978-1-4615-3476-1_39)
- Franchini, A. G., Henneberger, R., Aeppli, M., & Zeyer, J. (2014). Methane dynamics in an alpine fen: A field-based study on methanogenic and methanotrophic microbial communities. *FEMS Microbiology Ecology*, 91(3). <https://doi.org/10.1093/femsec/fiu032>
- Freeman, C., Ostle, N. J., Fenner, N., & Kang, H. (2004). A regulatory role for phenol oxidase during decomposition in peatlands. *Soil Biology and Biochemistry*, 36(10), 1663–1667. <https://doi.org/10.1016/j.soilbio.2004.07.012>
- Freeman, C., Ostle, N., & Kang, H. (2001). An enzymic 'latch' on a global carbon store. *Nature*, 409(6817), 149. <https://doi.org/10.1038/35051650>
- Galand, P. E., Fritze, H., Conrad, R., & Yrjala, K. (2005). Pathways for methanogenesis and diversity of methanogenic archaea in three boreal peatland ecosystems. *Applied and Environmental Microbiology*, 71(4), 2195–2198. <https://doi.org/10.1128/AEM.71.4.2195-2198.2005>
- Harayama, S., Kok, M., & Neidle, E. L. (1992). Functional and evolutionary relationships among diverse oxygenases. *Annual Review of Microbiology*, 46(1), 565–601. <https://doi.org/10.1146/annurev.mi.46.100192.003025>
- Hattori, S., Kamagata, Y., Hanada, S., & Shoun, H. (2000). *Thermacetogenium phaeum* gen. nov., sp. nov., a strictly anaerobic, thermophilic, syntrophic acetate-oxidizing bacterium. *International Journal of Systematic and Evolutionary Microbiology*, 50(4), 1601–1609. <https://doi.org/10.1099/00207713-50-4-1601>
- Hawkes, J. A., Dittmar, T., Patriarca, C., Tranvik, L., & Bergquist, J. (2016). Evaluation of the orbitrap mass spectrometer for the molecular fingerprinting analysis of natural dissolved organic matter. *Analytical Chemistry*, 88(15), 7698–7704. <https://doi.org/10.1021/acs.analchem.6b01624>
- Hines, M. E., Duddleston, K. N., Rooney-Varga, J. N., Fields, D., & Chanton, J. P. (2008). Uncoupling of acetate degradation from methane formation in Alaskan wetlands: Connections to vegetation distribution. *Global Biogeochemical Cycles*, 22(2). <https://doi.org/10.1029/2006gb002903>
- Hodgkins, S. B., Tfaily, M. M., McCalley, C. K., Logan, T. A., Crill, P. M., Saleska, S. R., Rich, V. I., & Chanton, J. P. (2014). Changes in peat chemistry associated with permafrost thaw increase greenhouse gas production. *Proceedings of the National Academy of Sciences of the United States of America*, 111(16), 5819–5824. <https://doi.org/10.1073/pnas.1314641111>
- Hodgkins, S. B., Tfaily, M. M., Podgorski, D. C., McCalley, C. K., Saleska, S. R., Crill, P. M., Rich, V. I., Chanton, J. P., & Cooper, W. T. (2016). Elemental composition and optical properties reveal changes in dissolved organic matter along a permafrost thaw chronosequence in a subarctic peatland. *Geochimica et Cosmochimica Acta*, 187, 123–140. <https://doi.org/10.1016/j.gca.2016.05.015>
- Horn, M. A., Matthies, C., Küsel, K., Schramm, A., & Drake, H. L. (2003). Hydrogenotrophic methanogenesis by moderately acid-tolerant methanogens of a methane-emitting acidic peat. *Applied and Environmental Microbiology*, 69(1), 74. <https://doi.org/10.1128/AEM.69.1.74-83.2003>
- Huson, D. H., Beier, S., Flade, I., Górská, A., El-Hadidi, M., Mitra, S., Ruscheweyh, H.-J., & Tappu, R. (2016). MEGAN community edition – Interactive exploration and analysis of large-scale microbiome sequencing data. *PLOS Computational Biology*, 12(6), e1004957. <https://doi.org/10.1371/journal.pcbi.1004957>
- Jørgensen, C. J., Struwe, S., & Elberling, B. (2012). Temporal trends in N<sub>2</sub>O flux dynamics in a Danish wetland – Effects of plant-mediated gas transport of N<sub>2</sub>O and O<sub>2</sub> following changes in water level and soil mineral-N availability. *Global Change Biology*, 18(1), 210–222. <https://doi.org/10.1111/j.1365-2486.2011.02485.x>
- Keiluweit, M., Gee, K., Denney, A., & Fendorf, S. (2018). Anoxic microsites in upland soils dominantly controlled by clay content. *Soil Biology and Biochemistry*, 118, 42–50. <https://doi.org/10.1016/j.soilbio.2017.12.002>
- Keiluweit, M., Nico, P. S., Kleber, M., & Fendorf, S. (2016). Are oxygen limitations under recognized regulators of organic carbon turnover in upland soils? *Biogeochemistry*, 127(2), 157–171. <https://doi.org/10.1007/s10533-015-0180-6>
- Kielak, A. M., Barreto, C. C., Kowalchuk, G. A., van Veen, J. A., & Kuramae, E. E. (2016). The ecology of acidobacteria: Moving beyond genes and genomes. *Frontiers in Microbiology*, 7(744). <https://doi.org/10.3389/fmicb.2016.00744>
- Kotsyurbenko, O. R., Friedrich, M. W., Simankova, M. V., Nozhevnikova, A. N., Golyshin, P. N., Timmis, K. N., & Conrad, R. (2007). Shift from acetoclastic to H<sub>2</sub>-dependent methanogenesis in a West Siberian peat bog at low pH values and isolation of an acidophilic Methanobacterium strain. *Applied and Environmental Microbiology*, 73(7), 2344–2348. <https://doi.org/10.1128/AEM.02413-06>
- Kristensen, E., Ahmed, S. I., & Devol, A. H. (1995). Aerobic and anaerobic decomposition of organic matter in marine sediment: Which is fastest? *Limnology and Oceanography*, 40(8), 1430–1437. <https://doi.org/10.4319/lo.1995.40.8.1430>
- Kumar, R., Verma, H., Haider, S., Bajaj, A., Sood, U., Ponnusamy, K., Nagar, S., Shakarad, M. N., Negi, R. K., Singh, Y., Khurana, J. P., Gilbert, J. A., & Lal, R. (2017). Comparative genomic analysis reveals habitat-specific genes and regulatory hubs within the genus *Novosphingobium*. *mSystems*, 2(3), e00020-00017. <https://doi.org/10.1128/mSystems.00020-17>
- LaRowe, D. E., & Van Cappellen, P. (2011). Degradation of natural organic matter: A thermodynamic analysis. *Geochimica et Cosmochimica Acta*, 75(8), 2030–2042. <https://doi.org/10.1016/j.gca.2011.01.020>
- Lehmann, J., & Kleber, M. (2015). The contentious nature of soil organic matter. *Nature*, 528(7580), 60–68. <https://doi.org/10.1038/nature16069>
- Loisel, J., Gallego-Sala, A. V., Amesbury, M. J., Magnan, G., Anshari, G., Beilman, D. W., Benavides, J. C., Blewett, J., Camill, P., Charman, D. J., Chawchai, S., Hedgpeth, A., Kleinen, T., Korhola, A., Large, D., Mansilla, C. A., Müller, J., van Bellen, S., West, J. B., ... Wu, J. (2021). Expert assessment of future vulnerability of the global peatland carbon sink. *Nature Climate Change*, 11(1), 70–77. <https://doi.org/10.1038/s41558-020-00944-0>
- Longhi, D., Bartoli, M., Nizzoli, D., Laini, A., & Viaroli, P. (2016). Do oxic-anoxic transitions constrain organic matter mineralization in eutrophic freshwater wetlands? *Hydrobiologia*, 774(1), 81–92. <https://doi.org/10.1007/s10750-016-2722-x>
- Lozupone, C., Hamady, M., & Knight, R. (2006). UniFrac – An online tool for comparing microbial community diversity in a phylogenetic context. *BMC Bioinformatics*, 7(1), 371. <https://doi.org/10.1186/1471-2105-7-371>
- McGivern, B. B., Tfaily, M. M., Borton, M. A., Kosina, S. M., Daly, R. A., Nicora, C. D., Purvine, S. O., Wong, A. R., Lipton, M. S., Hoyt, D. W., Northen, T. R., Hagerman, A. E., & Wrighton, K. C. (2021). Decrypting bacterial polyphenol metabolism in an anoxic wetland

- soil. *Nature Communications*, 12(1), 2466. <https://doi.org/10.1038/s41467-021-22765-1>
- Megonigal, J. P., Hines, M. E., & Visscher, P. T. (2003). 8.08 - Anaerobic metabolism: Linkages to trace gases and aerobic processes. In H. D. Holland & K. K. Turekian (Eds.), *Treatise on geochemistry* (pp. 317–424). Pergamon.
- Morgan, R. M., Pihl, T. D., Nölling, J., & Reeve, J. N. (1997). Hydrogen regulation of growth, growth yields, and methane gene transcription in *Methanobacterium thermoautotrophicum* deltaH. *Journal of Bacteriology*, 179(3), 889. <https://doi.org/10.1128/jb.179.3.889-898.1997>
- Naughton, H. R., Keiluweit, M., Tfaily, M. M., Dynes, J. J., Regier, T., & Fendorf, S. (2021). Development of energetic and enzymatic limitations on microbial carbon cycling in soils. *Biogeochemistry*, 153(2), 191–213. <https://doi.org/10.1007/s10533-021-00781-z>
- O'Connell, C. S., Ruan, L., & Silver, W. L. (2018). Drought drives rapid shifts in tropical rainforest soil biogeochemistry and greenhouse gas emissions. *Nature Communications*, 9(1), 1348. <https://doi.org/10.1038/s41467-018-03352-3>
- Ohno, T., Sleighter, R. L., & Hatcher, P. G. (2016). Comparative study of organic matter chemical characterization using negative and positive mode electrospray ionization ultrahigh-resolution mass spectrometry. *Analytical and Bioanalytical Chemistry*, 408(10), 2497–2504. <https://doi.org/10.1007/s00216-016-9346-x>
- Ohta, Y., Nishi, S., Hasegawa, R., & Hatada, Y. (2015). Combination of six enzymes of a marine *Novosphingobium* converts the stereoisomers of beta-O-4 lignin model dimers into the respective monomers. *Scientific Reports*, 5. <https://doi.org/10.1038/srep15105>
- Page, S. E., Kling, G. W., Sander, M., Harrold, K. H., Logan, J. R., McNeill, K., & Cory, R. M. (2013). Dark formation of hydroxyl radical in Arctic soil and surface waters. *Environmental Science & Technology*, 47(22), 12860–12867. <https://doi.org/10.1021/es4033265>
- Patra, A. K., & Saxena, J. (2010). A new perspective on the use of plant secondary metabolites to inhibit methanogenesis in the rumen. *Phytochemistry*, 71(11), 1198–1222. <https://doi.org/10.1016/j.phytochem.2010.05.010>
- Pedregosa, F., Varoquaux, G., Gramfort, A., Michel, V., Thirion, B., Grisel, O., Blondel, M., Prettenhofer, P., Weiss, R., Dubourg, V., Vanderplas, J., Passos, A., Cournapeau, D., Brucher, M., Perrot, M., & Duchesnay, É. (2011). Scikit-learn: Machine learning in python. *Journal of Machine Learning Research*, 12, 2825–2830.
- Pracht, L. E., Tfaily, M. M., Ardisson, R. J., & Neumann, R. B. (2018). Molecular characterization of organic matter mobilized from Bangladeshi aquifer sediment: Tracking carbon compositional change during microbial utilization. *Biogeosciences*, 15(6), 1733–1747. <https://doi.org/10.5194/bg-15-1733-2018>
- Price, M. N., Dehal, P. S., & Arkin, A. P. (2010). Fasttree 2—approximately maximum-likelihood trees for large alignments. *PLoS ONE*, 5(3), e9490. <https://doi.org/10.1371/journal.pone.0009490>
- Ravel, B., & Newville, M. (2005a). ATHENA and ARTEMIS: Interactive graphical data analysis using IFEFFIT. *Physica Scripta*, T115, 1007–1010. <https://doi.org/10.1238/Physica.Topical.115a01007>
- Ravel, B., & Newville, M. (2005b). ATHENA, ARTEMIS, HEPHAESTUS: Data analysis for X-ray absorption spectroscopy using IFEFFIT. *Journal of Synchrotron Radiation*, 12, 537–541. <https://doi.org/10.1107/s0909049505012719>
- Rooney-Varga, J. N., Giewat, M. W., Duddleston, K. N., Chanton, J. P., & Hines, M. E. (2007). Links between archaeal community structure, vegetation type and methanogenic pathway in Alaskan peatlands. *FEMS Microbiology Ecology*, 60, 240–251. <https://doi.org/10.1111/j.1574-6941.2007.00278.x>
- Rose, A. L., & Waite, T. D. (2003). Effect of dissolved natural organic matter on the kinetics of ferrous iron oxygenation in seawater. *Environmental Science & Technology*, 37(21), 4877–4886. <https://doi.org/10.1021/es034152g>
- Schmidt, M. W. I., Torn, M. S., Abiven, S., Dittmar, T., Guggenberger, G., Janssens, I. A., & Trumbore, S. E. (2011). Persistence of soil organic matter as an ecosystem property. *Nature*, 478(7367), 49–56. <https://doi.org/10.1038/nature10386>
- Shoemaker, J. K., & Schrag, D. P. (2010). Subsurface characterization of methane production and oxidation from a New Hampshire wetland. *Geobiology*, 8(3), 234–243. <https://doi.org/10.1111/j.1472-4669.2010.00239.x>
- Shoemaker, J. K., Varner, R. K., & Schrag, D. P. (2012). Characterization of subsurface methane production and release over 3 years at a New Hampshire wetland. *Geochimica et Cosmochimica Acta*, 91, 120–139. <https://doi.org/10.1016/j.gca.2012.05.029>
- Sinsabaugh, R. L. (2010). Phenol oxidase, peroxidase and organic matter dynamics of soil. *Soil Biology and Biochemistry*, 42(3), 391–404. <https://doi.org/10.1016/j.soilbio.2009.10.014>
- Sleighter, R. L., Chen, H., Wozniak, A. S., Willoughby, A. S., Caricasole, P., & Hatcher, P. G. (2012). Establishing a measure of reproducibility of ultrahigh-resolution mass spectra for complex mixtures of natural organic matter. *Analytical Chemistry*, 84(21), 9184–9191. <https://doi.org/10.1021/ac3018026>
- Sleighter, R. L., & Hatcher, P. G. (2008). Molecular characterization of dissolved organic matter (DOM) along a river to ocean transect of the lower Chesapeake Bay by ultrahigh resolution electrospray ionization Fourier transform ion cyclotron resonance mass spectrometry. *Marine Chemistry*, 110(3), 140–152. <https://doi.org/10.1016/j.marchem.2008.04.008>
- Teh, Y. A., Silver, W. L., & Conrad, M. E. (2005). Oxygen effects on methane production and oxidation in humid tropical forest soils. *Global Change Biology*, 11(8), 1283–1297. <https://doi.org/10.1111/j.1365-2486.2005.00983.x>
- Tfaily, M. M., Wilson, R. M., Cooper, W. T., Kostka, J. E., Hanson, P., & Chanton, J. P. (2018). Vertical stratification of peat pore water dissolved organic matter composition in a peat bog in northern Minnesota. *Journal of Geophysical Research: Biogeosciences*, 123(2), 479–494. <https://doi.org/10.1002/2017JG004007>
- Thauer, R., Kaster, A., Seedorf, H., Buckel, W., & Hedderich, R. (2008). Methanogenic archaea: Ecologically relevant differences in energy conservation. *Nature Reviews Microbiology*, 6(8), 579–591. <https://doi.org/10.1038/nrmicro1931>
- Tirola, M. A., Männistö, M. K., Puhakka, J. A., & Kulomaa, M. S. (2002). Isolation and characterization of *Novosphingobium* sp. strain MT1, a dominant polychlorophenol-degrading strain in a groundwater bioremediation system. *Applied and Environmental Microbiology*, 68(1), 173. <https://doi.org/10.1128/AEM.68.1.173-180.2002>
- Trusiak, A., Treibergs, L. A., Kling, G. W., & Cory, R. M. (2018). The role of iron and reactive oxygen species in the production of CO<sub>2</sub> in arctic soil waters. *Geochimica et Cosmochimica Acta*, 224, 80–95. <https://doi.org/10.1016/j.gca.2017.12.022>
- Turetsky, M. R., Kotowska, A., Bubier, J., Dise, N. B., Crill, P., Hornibrook, E. R. C., Minkinen, K., Moore, T. R., Myers-Smith, I. H., Nykänen, H., Olefeldt, D., Rinne, J., Saarnio, S., Shurpali, N., Tuittila, E.-S., Waddington, J. M., White, J. R., Wickland, K. P., & Wilkening, M. (2014). A synthesis of methane emissions from 71 northern, temperate, and subtropical wetlands. *Global Change Biology*, 20(7), 2183–2197. <https://doi.org/10.1111/gcb.12580>
- Turner, A. J., Frankenberg, C., & Kort, E. A. (2019). Interpreting contemporary trends in atmospheric methane. *Proceedings of the National Academy of Sciences of the United States of America*, 116(8), 2805. <https://doi.org/10.1073/pnas.1814297116>
- von der Heyden, B. P., Roychoudhury, A. N., Tyliczszak, T., & Myneni, S. C. B. (2017). Investigating nanoscale mineral compositions: Iron L-3-edge spectroscopic evaluation of iron oxide and oxy-hydroxide coordination. *American Mineralogist*, 102(3), 674–685. <https://doi.org/10.2138/am-2017-5805>
- Waggoner, D. C., Wozniak, A. S., Cory, R. M., & Hatcher, P. G. (2017). The role of reactive oxygen species in the degradation of lignin derived

- dissolved organic matter. *Geochimica et Cosmochimica Acta*, 208, 171–184. <https://doi.org/10.1016/j.gca.2017.03.036>
- Wakeham, S. G., & Canuel, E. A. (2006). Degradation and preservation of organic matter in marine sediments. In J. K. Volkman (Ed.), *Marine organic matter: Biomarkers, isotopes and DNA* (pp. 295–321). Springer Berlin Heidelberg. <https://doi.org/10.1007/b11682>
- Wozniak, A. S., Goranov, A. I., Mitra, S., Bostick, K. W., Zimmerman, A. R., Schlesinger, D. R., Myneni, S., & Hatcher, P. G. (2020). Molecular heterogeneity in pyrogenic dissolved organic matter from a thermal series of oak and grass chars. *Organic Geochemistry*, 148. <https://doi.org/10.1016/j.orggeochem.2020.104065>
- Yang, W. H., McNicol, G., Teh, Y. A., Estera-Molina, K., Wood, T. E., & Silver, W. L. (2017). Evaluating the classical versus an emerging conceptual model of peatland methane dynamics. *Global Biogeochemical Cycles*, 31(9), 1435–1453. <https://doi.org/10.1002/2017GB005622>
- Zak, D., Roth, C., Unger, V., Goldhammer, T., Fenner, N., Freeman, C., & Jurasinski, G. (2019). Unraveling the importance of polyphenols for microbial carbon mineralization in rewetted riparian peatlands. *Frontiers in Environmental Science*, 7(147). <https://doi.org/10.3389/fenvs.2019.00147>
- Zhang, J. J., Kobert, K., Flouri, T., & Stamatakis, A. (2014). PEAR: A fast and accurate Illumina Paired-End reAd mergeR. *Bioinformatics*, 30(5), 614–620. <https://doi.org/10.1093/bioinformatics/btt593>
- Zhang, Z., Zimmermann, N. E., Stenke, A., Li, X., Hodson, E. L., Zhu, G., Huang, C., & Poulter, B. (2017). Emerging role of wetland methane emissions in driving 21st century climate change. *Proceedings of the National Academy of Sciences of the United States of America*, 114(36), 9647–9652. <https://doi.org/10.1073/pnas.1618765114>

## SUPPORTING INFORMATION

Additional Supporting Information may be found online in the Supporting Information section.

**How to cite this article:** Wilmoth, J. L., Schaefer, J. K., Schlesinger, D. R., Roth, S. W., Hatcher, P. G., Shoemaker, J. K., & Zhang, X. (2021). The role of oxygen in stimulating methane production in wetlands. *Global Change Biology*, 27, 5831–5847. <https://doi.org/10.1111/gcb.15831>